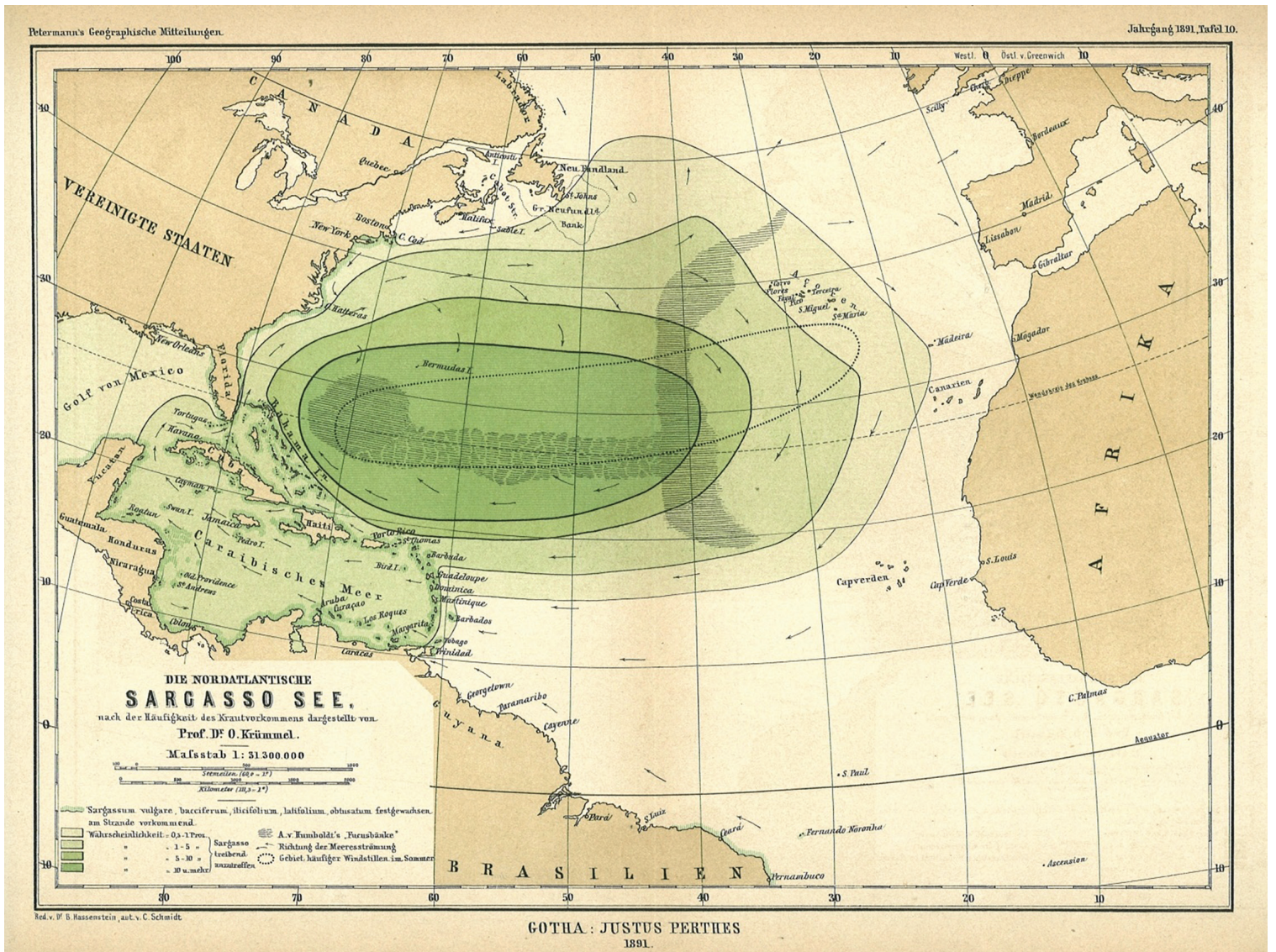


# Preparatory Data Discovery and Analysis to Support Enhanced Management and Governance of the Sargasso Sea: A Description of the Feature in Space and Time

Jesse Cleary, Beatrice Smith, Nathan Ellermeier, Ei Fujioka, Ben Donnelly, Sarah DeLand, Connie Kot, Corrie Curtice, Pat Halpin

Otto Krümmel



A Report Submitted to Sargasso Sea Commission



The Sargasso Sea Commission works to “encourage and facilitate voluntary collaboration toward the conservation of the Sargasso Sea.” The Hamilton Declaration on Collaboration for the Conservation of the Sargasso Sea, established in 2014, provides a framework for voluntary collaboration between ten signatory governments and a Commission of scientific experts operating in their independent capacities for the conservation of the Sargasso Sea.

This work is an underlying report to the Socio-Ecosystem Diagnostic Analysis (SEDA) for the Sargasso Sea—the first analysis of its kind of a high seas ecosystem.

This work was funded under two separate but complementary projects of the Sargasso Sea Commission, the Global Environment Facility funded Sargasso Sea project (GEF-UNDP-IOC-SSC), a child project of the Common Oceans Program, implemented by UNDP and executed by IOC-UNESCO, and the French Facility for Global Environment funded ‘SARGADOM’ project in partnership with the University of Western Brittany and Mar Viva.

Further details: The Secretariat of the Sargasso Sea Commission is hosted by the Washington D.C. Office of the International Union for the Conservation of Nature (IUCN), Suite 300, 1630 Connecticut Avenue NW, Washington D.C., 2009, USA.

A full version of this report and of the reports commissioned by the SSC are available for download on the website at [www.sargassoseacommission.org](http://www.sargassoseacommission.org)

For further details contact:

Dr David Freestone (Executive Secretary) at [dfreestone@sargassoseacommission.org](mailto:dfreestone@sargassoseacommission.org) or  
Fae Sapsford (Communications Officer) at [fsapsford@sargassoseacommission.org](mailto:fsapsford@sargassoseacommission.org)

# Preparatory Data Discovery and Analysis to Support Enhanced Management and Governance of the Sargasso Sea: A Description of the Feature in Space and Time



A Report Submitted to Sargasso Sea Commission

---

## Table of Contents

List of Figures .....	5
List of Tables.....	6
Preparatory Data Discovery and Analysis to Support Enhanced Management and Governance of the Sargasso Sea: A Description of the Feature in Space and Time .....	7
Introduction .....	7
Background.....	7
Project Overview .....	8
Past Work.....	8
Methodology .....	10
Temporal and Spatial Extent.....	10
Study region .....	10
Data Resources and Summarization.....	11
Sub-Region Detection.....	22
Results .....	25
Discussion and Conclusion.....	29
Literature Cited.....	32

## List of Figures

Figure 1. Possible Sargasso Sea sub-region delineation, figure 10 from Ardron et al., 2011.....	8
Figure 2. Possible Sargasso Sea sub-region delineation, figure 11 from Ardron et al., 2011 .....	9
Figure 3. Map of the Sargasso Sea EBSA from the 2012 CBD EBSA workshop.....	9
Figure 4. Map of the Sargasso Sea Geographical Area of Collaboration .....	9
Figure 5. Mean current speed (top) and direction (bottom) for the Sargasso Sea region over the complete study period.....	12
Figure 6. Mean monthly current speed (m/s) for the Sargasso Sea.....	12
Figure 7. Mean monthly current direction (°) for the Sargasso Sea region.....	13
Figure 8. Current streamlines for the Sargasso Sea region over the complete study period. Streamlines symbolized in lighter colors reflect greater magnitude, with arrows showing directionality of the currents.....	13
Figure 9. Monthly cyclonic Eddy count for the Sargasso Sea region over the complete study period. ....	14
Figure 10. Monthly anticyclonic eddy count for the Sargasso Sea region for each month of the year. ....	15
Figure 11. Anticyclonic (lower) and eddy (upper) eddy count for the Sargasso Sea region over the complete study period.....	15
Figure 12. Mean absolute dynamic topography over the study period.....	16
Figure 13. Mean monthly absolute dynamic topography.....	16
Figure 14. Mean salinity for the entire study period.....	17
Figure 15. Mean monthly salinity.....	17
Figure 16. Mean chlorophyll-a concentration across the study period.....	18
Figure 17. Mean monthly chlorophyll-a concentration.....	18
Figure 18. Mean sea surface temperature across the study period.....	19
Figure 19. Mean monthly sea surface temperature.....	19
Figure 20. Monthly thickness of Subtropical Mode Water in the Sargasso Sea defined as water with a temperature between 17.5°C and 18.5 °C.....	20
Figure 21. Monthly sea surface temperature front count.....	21
Figure 22. Monthly mode of seascape pelagic habitats for the study region.....	23
Figure 23. Decision tree classification matrix including decision rule criteria for each variable. ....	24
Figure 24. Major currents relative to the Geographical Area of Collaboration (top) and decision tree classification of the study area (bottom).....	26
Figure 25. Monthly decision tree classification of the study region.....	27
Figure 26. Mode class of monthly decision tree classification (above) and mode frequency (below). Areas with a higher mode frequency, or count, reflect those of increased stability throughout the year and lower seasonal variation.....	28

---

## List of Tables

Table 1. Catalog of datasets used for description of feature in space and time. ....	11
Table 2. Seascape pelagic habitat classes represented in the study area and corresponding descriptions. ....	22
Table 3. Description of each sub-region class as defined by the supervised decision tree classification.....	26

# Preparatory Data Discovery and Analysis to Support Enhanced Management and Governance of the Sargasso Sea: A Description of the Feature in Space and Time

## Introduction

### Background

The Sargasso Sea (SS) is an area of the western North Atlantic Ocean where mats of *Sargassum* seaweed (primarily *S.natans* and *S. fluitans*) aggregate, forming what many refer to as a “floating rainforest”. The Sargasso Sea is located at the heart of the North Atlantic Gyre, which is made up of several circulating currents including the Gulf Stream, the Azores Current, the Canary Current, the North Equatorial Current, and the Antilles Current (Figure 3). Typical of many oceanic gyres in the northern hemisphere, the western currents of this system are more concentrated and easily discernable than those at the eastern extent. Thus, there is a fairly strong boundary on the western side of the SS, with a more moderate one to the north and south, and a relatively weak bounding effect from those currents found in the eastern extent of the study area. The Sargasso Sea is also influenced by a series of rings and eddies, together known as mesoscale eddies, that can persist for months to years at a time and play a central role in temperature regulation, salinity and nutrient concentration, and *Sargassum* mat aggregation (Benitez-Nelson and McGillicuddy, 2008). It is through this system of currents and eddies that *Sargassum* is transported from the Caribbean, traveling into the Gulf of Mexico and up the eastern seaboard of the United States entrained in the Gulf Stream, then trapped within the North Atlantic Gyre and concentrated by eddies.

The Sargasso Sea provides a rare mosaic of valuable and protective habitat in the deep water of the open ocean. With a high degree of persistence and a wide-spread footprint, this thick layer of *Sargassum* attracts a diverse and abundant species assemblage, distinguishing it from any other drift algae (Coston-Clements et al., 1991; Casazza and Ross 2008). There are ten species known to be endemic to floating *Sargassum* including the Sargassum crab (*Planes minutes*), Sargassum pipefish (*Syngnathus pelagicus*), and the Sargassum anemone (*Anemonia sargassensis*), to name a few. Additionally, the SS provides valuable habitat to several species of high

conservation value. This feature acts as the spawning area for the economically valuable American and European eels (*Anguilla rostrata* and *A. anguilla*) which spend their adult lives in freshwater but migrate thousands of miles to the SS to spawn (Kleckner et al., 1983; Friedland et al., 2007). Larval development occurs in the SS, after which both species migrate along the Gulf Stream back to freshwater habitats in North America and Europe where they metamorphose into their juvenile forms, referred to as “glass eels”. As an economically valuable species, there is growing international concern over the severe decline of glass eel recruitment, with populations of both species suffering from significant population reduction.

Several species of turtles, all of which are endangered or critically endangered, spend time as hatchlings and juveniles in the protective layer of the Sargasso Sea. Green turtles (*Chelonia mydas*), hawksbill turtles (*Eretmochelys imbricate*), loggerhead turtles (*Caretta caretta*), and Kemp’s Ridley turtles (*Lepidochelys kempii*), all use the *Sargassum* as a nursery habitat (Carr and Meylan 1980; Carr, 1987), spending their ‘lost years’ feeding and sheltering in this area. For these, as well as many other species, the *Sargassum* mats provide a stable structure habitat with a rich food supply, protection from predators and thermal regulation that promotes growth and feeding (Mansfield et al., 2014; Mansfield et al., 2021). In fact, the Sargasso Sea acts as a nursery and spawning habitat for many other species including swordfish (*Xiphias gladius*), dolphinfish (*Coryphaenidae* spp.), flying fish (*Exocoetidae* spp.), and blue marlin (*Makaira nigricans*) (Casazza and Ross, 2008; Dooley, 1972; Luckhurst et al., 2006; South Atlantic Fishery Management Council, 2002)

In addition to acting as spawning and nursery habitat for a wide array of species, the Sargasso Sea is a stopover and feeding site for many others. A number of pelagic fish species including Atlantic bluefin tuna (*Thunnus thynnus*) and Atlantic swordfish (*Xiphias gladius*), both of which are economically important, move through this area (Block et al., 2001; Loefer et al., 2007). Sharks and rays also make use of the Sargasso Sea, inhabiting or migrating through the Sargasso Sea seasonally. For example, basking sharks

(*Cetorhinus maximus*) regularly move through the this area during winter months at depths of 200 – 1000 m (Skomal et al., 2009). Moreover, as many as 30 cetacean species have been observed in and around the Sargasso Sea. Humpback whales (*Megaptera novaeangliae*) routinely pass through this area during annual migrations and sperm whales (*Physeter catodon*) are commonly observed as well, with adults and calves likely feeding at the frontal convergence and around the boundaries of the Gulf Stream (National Marine Fisheries Services, 2010).

The Sargasso Sea provides widespread support to biodiversity and ecosystem health and even aids in global carbon sequestration (Laffoley et al., 2011). The socio-economic and cultural significance of this feature is significant, and it is important to enhance understanding of its spatio-temporal behavior to design and implement impactful conservation measures. This report explores data sources, summarization and synthesis methodologies to address existing gaps in this area, with the central purpose of delineating boundaries that are relevant and useful to conservation and management initiatives.

**Project Overview**

The descriptive analysis of the Sargasso Sea’s spatio-temporal dynamics is part of a larger project funded by Le Fond Français pour l’Environnement Mondial (<https://www.ffem.fr>) and coordinated by the Sargasso Sea Commission (<http://www.sargassoseacommission.org/>) aimed at constructing a more complete profile of the environmental, oceanographic, biological, ecosystem health, and human use pressures of this feature. This project has three parts: 1) Describe the dynamic Sargasso Sea feature

and its spatio-temporal variability 2) Review the data and information needs for the Ecosystem Diagnostic Analysis (EDA) 3) Analyze and synthesize existing research and information. Ultimately, the information provided here will become part of a greater analysis and synthesis effort (referred to here as the EDA) to allow stakeholders (managers, trainers, policy experts etc.) to assess possible management and governance improvements for the Sargasso Sea. This effort is guided by a Driver-Pressure-State-Impact-Response (DPSIR) framework developed by project partners, which has helped to inform identification of data resources and drive analysis and synthesis.

**Past Work**

This work builds upon previous research on the Sargasso Sea boundaries from the Sargasso Sea Alliance starting in 2010 and examination through the Convention on Biological Diversity Ecologically or Biologically Significant Marine Areas (CBD EBSA) process in 2012.

The Sargasso Sea Alliance supported research on the Sargasso Sea beginning in 2010 (Ardrón et al. 2011). This report explored and synthesized datasets relevant to the oceanographic context of the region and movement and remote sensing of Sargassum. This report resulted in the elliptical boundary for the Sargasso Sea Study Area as a general boundary for the area of ecological importance in the region. The report also described possible sub-regions within and surrounding this central area. One of the three core recommendations of this report was that more work be done on a biogeographic classification of the region and surrounding North Atlantic Gyre.

This elliptical boundary was also used in the

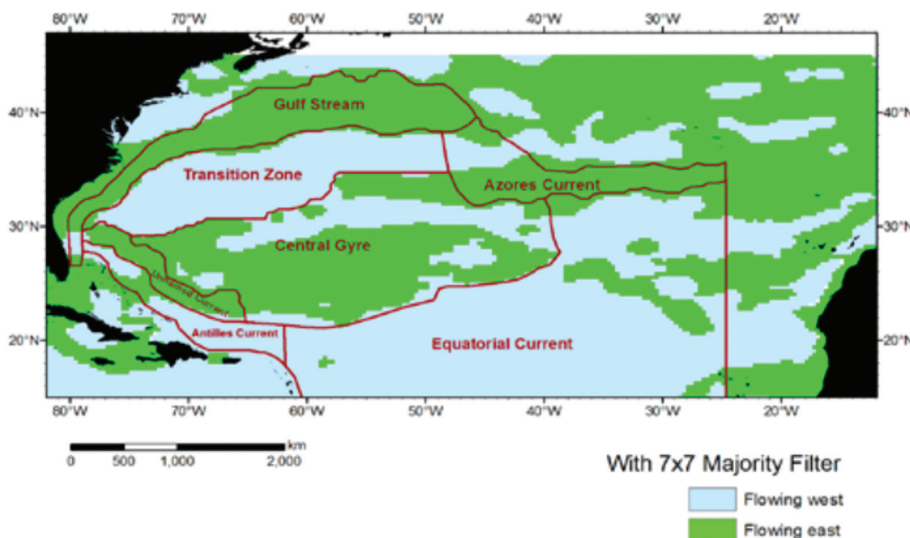


**FIGURE 1.** Possible Sargasso Sea sub-region delineation, figure 10 from Ardrón et al., 2011

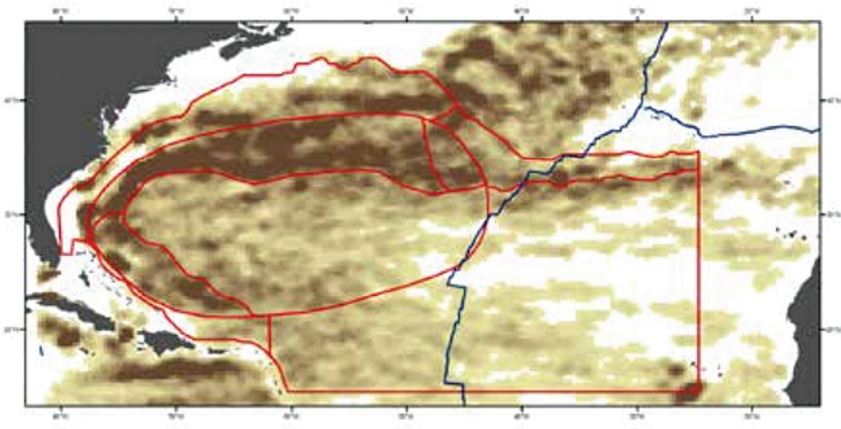


**FIGURE 2.** Possible Sargasso Sea sub-region delineation, figure 11 from Ardron et al., 2011

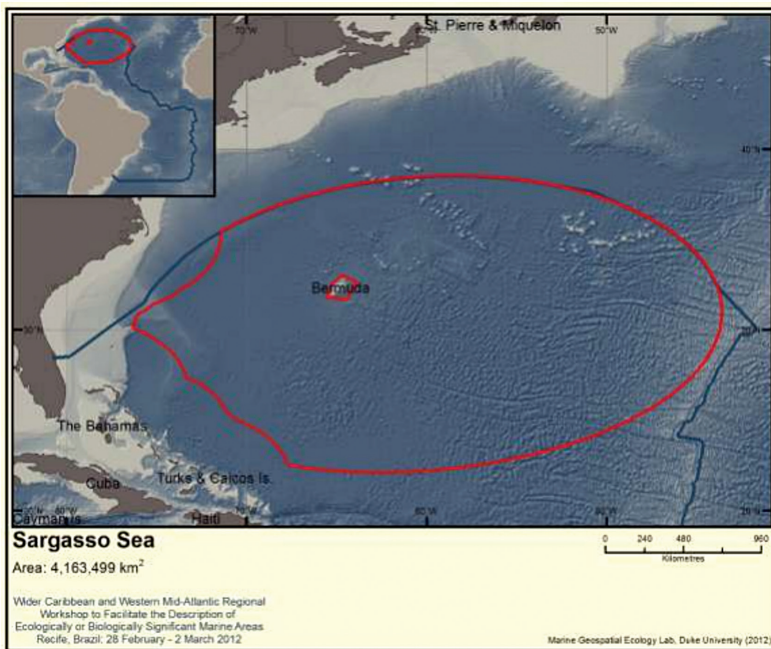


**FIGURE 3.** Map of the Sargasso Sea EBSA from the 2012 CBD EBSA workshop

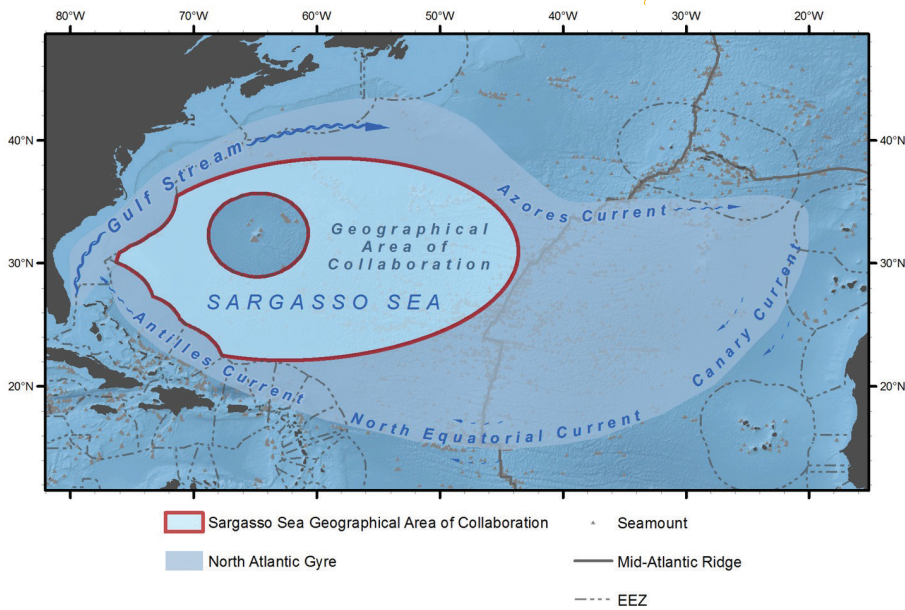


**FIGURE 4.** Map of the Sargasso Sea Geographical Area of Collaboration

description of the Sargasso Sea as a marine area of Ecological or Biological Significance (EBSA) in the “Wider Caribbean and Western Mid-Atlantic Regional Workshop to Facilitate the Description of Ecologically or Biologically Significant Marine Areas” held in Recife, Brazil in 2012 (CBD, 2012).

This elliptical boundary was further modified following the formation of the Sargasso Sea Commission and is now referred to as the Sargasso Sea Geographical Area of Collaboration. This boundary appears on the maps in this report as spatial context from these previous efforts.

## Methodology

The process for describing the Sargasso Sea in space and time included several central steps:

1. Identification of existing resources for oceanographic and climatological data in the region
2. Determination of the temporal and spatial extent of analyses
3. Paring down of datasets for further analyses and syntheses
4. Summarization of focal datasets at various temporal resolutions
5. Testing of various methodologies for sub-region delineation using data summarizations
5. Finalization of sub-regions analysis methodology and application of this method to overall and monthly time steps

These analyses were performed using a combination of RStudio (version 22.07.2, RStudio Team, 2020), ArcGIS Pro (version 2.8.8) or Visual Studio Code (version 1.70.2).

### Temporal and Spatial Extent

The temporal range of this project spanned from 2010-2019 inclusive, making for ten complete years of data for each environmental variable. This time span was chosen in large part due to data availability, with the objective of determining a timespan covered by all variables included in our analyses and taking into account our focus on the more recent past in order to assess the contemporary spatio-temporal behavior of the feature.

Additionally, data were summarized using two temporal resolutions: an overall summarization and monthly climatologies. The overall summarization is the calculation of metrics such as a mean, median or sum from data points across the entire study period and represents a baseline value of conditions for a given variable. The

monthly climatology includes calculation of metrics from data across the entire 10-year study period grouped by month, which provides insight into seasonality of environmental variables within the region.

### Study region

The study region was established in consultation with the SARGADOM project leads. The area was intentionally broad to capture any contextual oceanographic features or human patterns in adjacent areas, such as the Gulf Stream current system and Canary current system. The study region extends from 15°N to 45°N and from 25°W to 82°W. A modified Mollweide projection was selected for any area calculations that require an equal-area map projection.

For spatial context, the map products presented below include the Sargasso Sea Geographical Area of Collaboration polygon used by the Sargasso Sea Commission.

### Currents

Currents are a central driver of ecological dynamics found in Sargasso Sea with major current systems in the area including the Gulf Stream, the Azores Current, the Northern Equatorial Current and the Antilles Current (Figure 3). Several of these currents play a role in the larger circulating system known as the North Atlantic Gyre. Towards the western side of the Gyre (along the East Coast of the United States and the West Indies), the bounding currents of this system are more concentrated and therefore create a more easily discernable boundary than the eastern edge, where currents are more dispersed and weaker. Thus, to the west and north the Sargasso Sea is bounded by the Gulf Stream, to the south by the Northern Equatorial/Antilles currents and to the East by the Azores/Northern Equatorial currents. Given the importance of circulating currents within this study region and their impact on both abiotic and biotic conditions within the Sargasso Sea, this report summarizes current dynamics in two ways and incorporates both variables into our sub-region analysis.

#### Surface currents

Mean monthly surface current magnitude and direction were summarized from the NOAA Drifter-Derived Climatology of Global Near-Surface Currents (Laurindo et al., 2017), which includes a climatology of near-surface currents and temperatures for the world at monthly and one-quarter degree resolution, derived from satellite-tracked surface drifting buoy observations. This

## Data Resources and Summarization

TABLE 1. Catalog of datasets used for description of feature in space and time.

Dataset	Citation	Variables Used	Access	Temporal Resolution	Spatial Resolution
<b>CMEMS-SLA</b>	Taburet, G., Sanchez-Roman, A., Ballarotta, M., Pujol, M.-I., Legeais, J.-F., Fournier, F., Faugere, Y., and Dibarboure, G.: DUACS DT2018: 25 years of reprocessed sea level altimetry products, <i>Ocean Sci.</i> , 15, 1207–1224, <a href="https://doi.org/10.5194/os-15-1207-2019">https://doi.org/10.5194/os-15-1207-2019</a> (external to C3S), 2019.	Absolute dynamic topography	<a href="https://cds.climate.copernicus.eu/cdsapp#!/dataset/satellite-sea-level-global?tab=overview">https://cds.climate.copernicus.eu/cdsapp#!/dataset/satellite-sea-level-global?tab=overview</a>	Daily	0.25 degree gridded
<b>Global Mesoscale Eddy Trajectory Atlas</b>	Pegliasco, C., Delepoulle, A., Mason, E., Morrow, R., Faugère, Y., Dibarboure, G., 2022. META3.1exp: a new global mesoscale eddy trajectory atlas derived from altimetry. <i>Earth Syst. Sci. Data</i> 14, 1087–1107. <a href="https://doi.org/10.5194/essd-14-1087-2022">https://doi.org/10.5194/essd-14-1087-2022</a>	Cyclonic and anti-cyclonic eddy detection	<a href="https://www.aviso.altimetry.fr/en/home.html">https://www.aviso.altimetry.fr/en/home.html</a>	Daily	NA
<b>Hybrid Coordinate Ocean Model (HYCOM)</b>	J. A. Cummings and O. M. Smedstad. 2013: Variational Data Assimilation for the Global Ocean. <i>Data Assimilation for Atmospheric, Oceanic and Hydrologic Applications</i> vol II, chapter 13, 303-343.	Salinity	<a href="https://developers.google.com/earth-engine/datasets/catalog/HYCOM_sea_temp_salinity">https://developers.google.com/earth-engine/datasets/catalog/HYCOM_sea_temp_salinity</a>	3 hour	.08 degree gridded
<b>Ecological Marine Units</b>	Wright, D., Sayre, R., Breyer, S., Butler, K., VanGraafeiland, K., Costello, M., Goodin, K., Kavanaugh, M., Cressie, N., Basher, Z., Harris, P., & Guinotte, J. (2018, March 30). Ecological Marine Units as a Framework for Collaborative Data Science and Knowledge Discovery (world) [Poster]. <i>Earth and Space Science Open Archive; Earth and Space Science Open Archive</i> . <a href="https://doi.org/10.1002/essoar.874304ea88e4d45a.2883ea4f6e0f4d89.1">https://doi.org/10.1002/essoar.874304ea88e4d45a.2883ea4f6e0f4d89.1</a>	EMU classification	<a href="https://www.esri.com/en-us/about/science/ecological-marine-units/overview">https://www.esri.com/en-us/about/science/ecological-marine-units/overview</a>		.25 degree gridded
<b>Moderate Resolution Imaging Spectroradiometer</b>	NASA Goddard Space Flight Center, Ocean Ecology Laboratory, Ocean Biology Processing Group. Moderate-resolution Imaging Spectroradiometer (MODIS) Aqua Ocean Color Data, NASA OB.DAAC, Greenbelt, MD, USA.	Chlorophyll A concentration	<a href="https://developers.google.com/earth-engine/datasets/catalog/NASA_OCEANDATA_MODIS-Aqua_L3SMI">https://developers.google.com/earth-engine/datasets/catalog/NASA_OCEANDATA_MODIS-Aqua_L3SMI</a>	Monthly	4.6 km (equator)
<b>MUR-GHRSSRT</b>	JPL MUR MeASURES Project. 2015. GHRSSRT Level 4 MUR Global Foundation Sea Surface Temperature Analysis. Ver. 4.1. PO.DAAC, CA, USA. Dataset accessed [YYYY-MM-DD] at <a href="https://doi.org/10.5067/GHGMR-4FJ04">https://doi.org/10.5067/GHGMR-4FJ04</a>	Sea Surface Temperature	<a href="https://podaac.jpl.nasa.gov/dataset/MUR-JPL-L4-GLOB-v4.1">https://podaac.jpl.nasa.gov/dataset/MUR-JPL-L4-GLOB-v4.1</a>	Hourly; Daily	.01 degree gridded
<b>NOAA Global Drifter Program</b>	Laurindo, L., A. Mariano, and R. Lumpkin, 2017: An improved near-surface velocity climatology for the global ocean from drifter observations <i>Deep-Sea Res. I</i> , 124, pp.73-92, doi:10.1016/j.dsr.2017.04.009.	Surface currents	<a href="https://www.aoml.noaa.gov/phod/gdp/mean_velocity.php">https://www.aoml.noaa.gov/phod/gdp/mean_velocity.php</a>	Monthly; annual	.25 degree gridded
<b>Sargassum Distribution</b>	Hu, C. (2009). A novel ocean color index to detect floating algae in the global oceans. <i>Remote Sensing of Environment</i> , 113(10), 2118–2129. <a href="https://doi.org/10.1016/j.rse.2009.05.012">https://doi.org/10.1016/j.rse.2009.05.012</a>  Wang M, Hu C (2016) Mapping and quantifying Sargassum distribution and coverage in the Central West Atlantic using MODIS observations. <i>Remote Sensing of Environment</i> 183:350–367.  Trinanes J, Putman NF, Goni G, Hu C, Wang M (2021) Monitoring pelagic Sargassum inundation potential for coastal communities. <i>Journal of Operational Oceanography</i> 0:1–12.	Floating Algae Index  Alternative Floating Algae Index  Maximum Chlorophyll Index	Various Remote Sensing Portals	Daily	Varies; as high as 300m for MCI from Sentinel 3
<b>Seascape Pelagic Habitat</b>	Kavanaugh, M.T., Oliver, M J., Chavez, F.P., Letelier, R.M., Muller-Karger, F.E., Doney, S.C. 2016. Seascapes as a new vernacular for ocean monitoring, management and conservation. <i>ICES Journal of Marine Science</i> . doi:10.1093/icesjms/fsw086 (link is external).	Pelagic Seascape Classification	<a href="https://coastwatch.noaa.gov/cw/satellite-data-products/multi-parameter-models/seascape-pelagic-habitat-classification.html">https://coastwatch.noaa.gov/cw/satellite-data-products/multi-parameter-models/seascape-pelagic-habitat-classification.html</a>	Monthly	5 km
<b>World Ocean Atlas</b>	Boyer, Tim P.; Garcia, Hernan E.; Locarnini, Ricardo A.; Zweng, Melissa M.; Mishonov, Alexey V.; Reagan, James R.; Weathers, Katharine A.; Baranova, Olga K.; Seidov, Dan; Smolyar, Igor V. (2018). <i>World Ocean Atlas 2018</i> . [indicate subset used]. NOAA National Centers for Environmental Information. Dataset. <a href="https://www.ncei.noaa.gov/archive/accession/NCEI-WOA18">https://www.ncei.noaa.gov/archive/accession/NCEI-WOA18</a> .	Ocean Temperature	<a href="https://www.ncei.noaa.gov/metadata/geoportal/rest/metadata/item/gov.noaa.nodc%3ANCEI-WOA18/html">https://www.ncei.noaa.gov/metadata/geoportal/rest/metadata/item/gov.noaa.nodc%3ANCEI-WOA18/html</a>	Monthly	.25 degree gridded

dataset includes annual and monthly climatologies of U (eastward speed in m/s) and V (northward speed in m/s). We calculated surface current magnitude (cm) as:

$$cm = \sqrt{u + v^2}$$

and current direction (cd) as

$$cd = \tan^{-1} v/u$$

which produces direction in radians. Direction in radians (cd<sub>r</sub>) was then converted to degrees (cd<sub>d</sub>) using

$$cd_d = \frac{cd_r}{\pi} \times 180$$

With direction given as degrees from due north. We calculated surface current magnitude (m/s) and direction (°) as an overall mean (Figure 5) as well as monthly mean climatologies (Figures 6 and 7). We also created stream plots to show mean monthly direction and magnitude together as velocity (Figure 8).

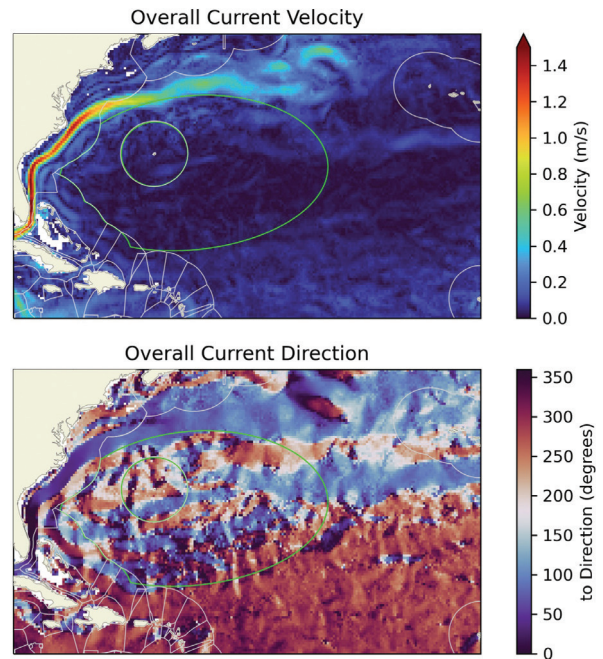


**FIGURE 5.** Mean current speed (top) and direction (bottom) for the Sargasso Sea region over the complete study period.

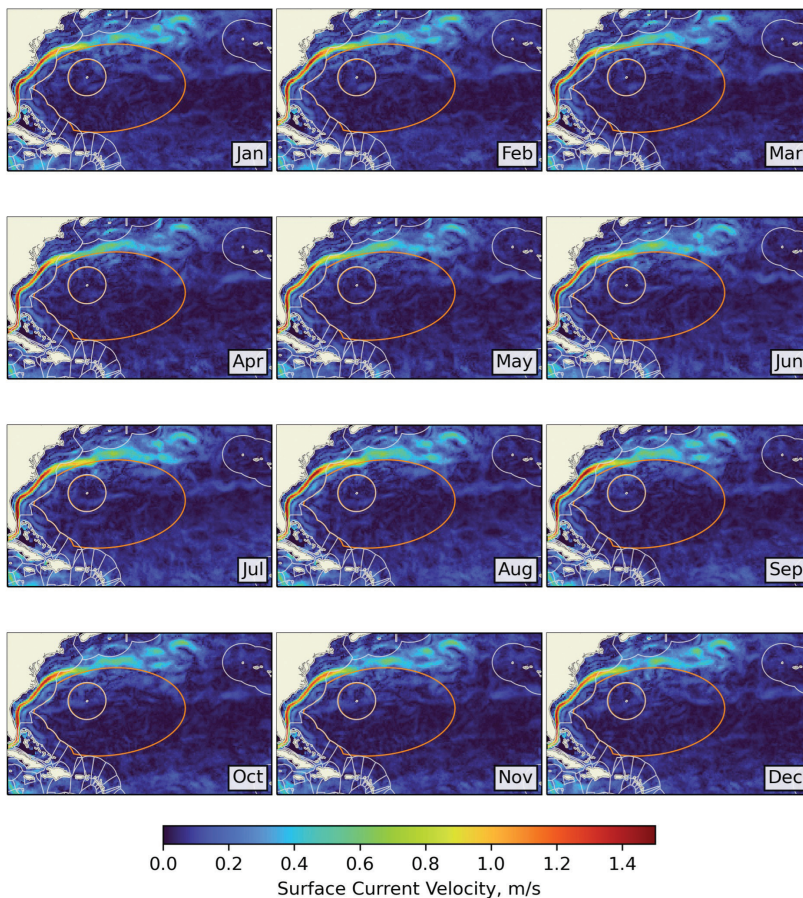


**FIGURE 6.** Mean monthly current speed (m/s) for the Sargasso Sea.

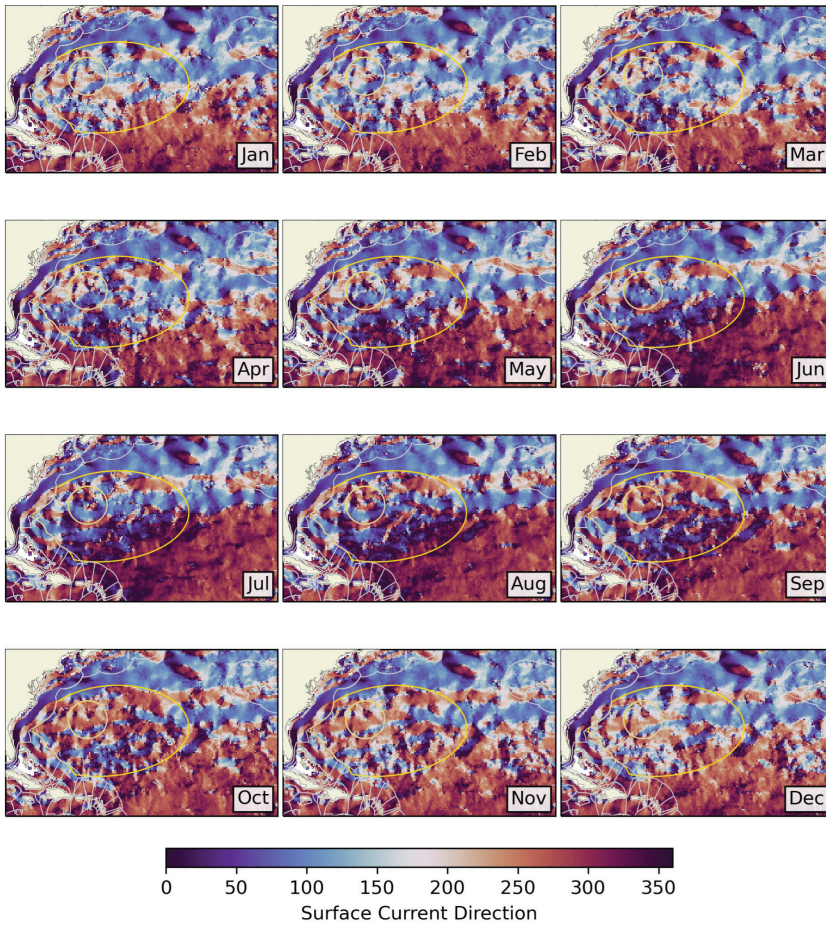


**FIGURE 7.** Mean monthly current direction ( $^{\circ}$ ) for the Sargasso Sea region.

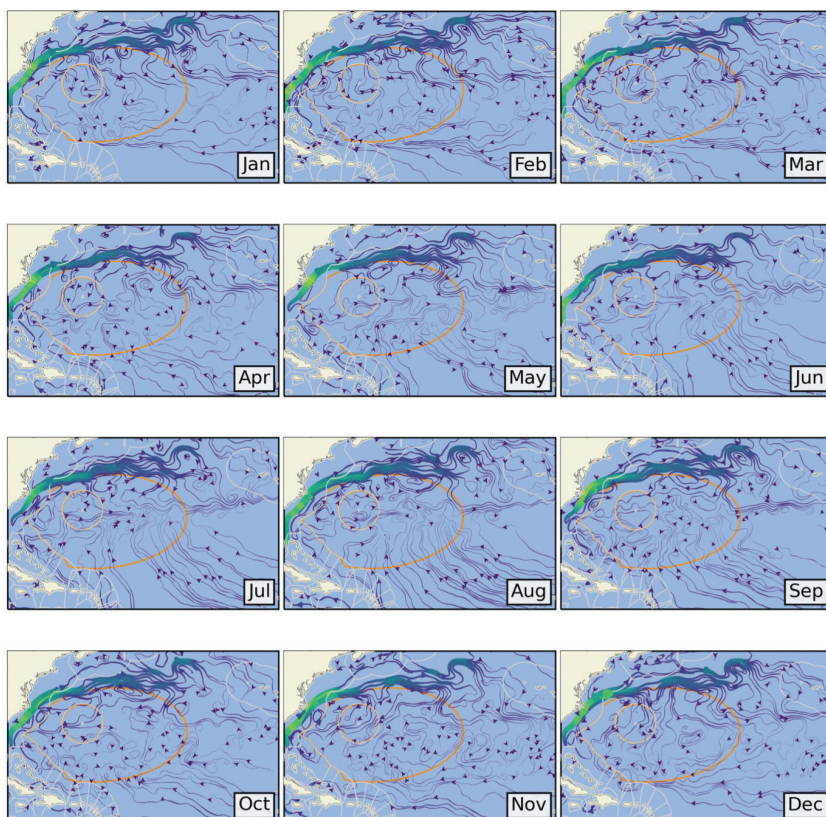


**FIGURE 8.** Current streamlines for the Sargasso Sea region over the complete study period. Streamlines symbolized in lighter colors reflect greater magnitude, with arrows showing directionality of the currents.

**Eddies**

The Gulf stream is a major source of eddies, circular currents of water produced by larger current systems, throughout the Northern Atlantic. Generally, eddies can be categorized into three types: mode water, cyclonic, otherwise known as cold core rings (Richardson et al., 1978), and anti-cyclonic. Cyclonic eddies are concentrated in the northern half of the study area (Cornillon et al., 1986) and rotate counterclockwise, encouraging upwelling that brings nutrients to the sea surface which promotes primary productivity and acts as an important ecological mechanism in the Sargasso Sea. Anticyclonic eddies rotate clockwise in the northern hemisphere, encouraging mixing as well as aggregation of materials. Anticyclonic eddies are less common in the study area but have a potentially significant ecological role as a mechanism for aggregating Sargassum into mats (Ardron et al., 2011).

This project implemented eddy data from the Global Mesoscale Eddy Trajectory Atlas (Pegliasco et al., 2022) accessed through the AVISO database, which provides anticyclonic and cyclonic eddies detected from multi-mission altimetry datasets, with their location, contours, amplitude, radius speed and associated metadata. Eddy data were subset to the study region using latitudinal and longitudinal coordinates and were included in the study region only if their centroid was within the area bounding

box, meaning that those eddies that had edges within the bounding box but centroids outside of the region were excluded from this analysis. We created an overall eddy density raster layer for each day of the sample period by generating an effective contour polygon for each eddy, rasterizing each of these polygons and adding them to a summary raster layer wherein each pixel value begins at 0 and increased in number each time it overlaps with an additional eddy polygon. We created both cyclonic and anticyclonic eddy count per pixel as monthly climatology (Figures 9 and 10) in which daily eddy count for all days belonging to the same month across the 10-year sample period were added together, giving a raster layer of total eddy count for each month of the year. We also calculated and overall eddy count raster (Figure 11) as the sum of all daily eddy counts for 365 days (1 year) for each of the ten years. It is important to note that we only included eddies that had a duration longer than 8 weeks, which we considered to be a minimum threshold for ecological influence upon the study area.

**Absolute Dynamic Topography**

This project incorporated absolute dynamic topography (ADT), a metric for measuring ocean levels, which is defined as the sea surface height above the geoid computed as the sum of the sea level anomaly with the mean

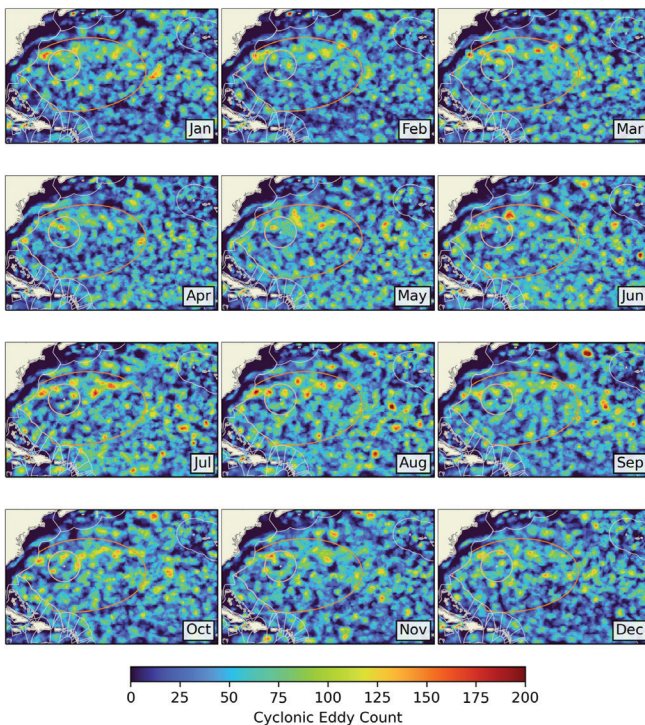


**FIGURE 9.** Monthly cyclonic Eddy count for the Sargasso Sea region over the complete study period.

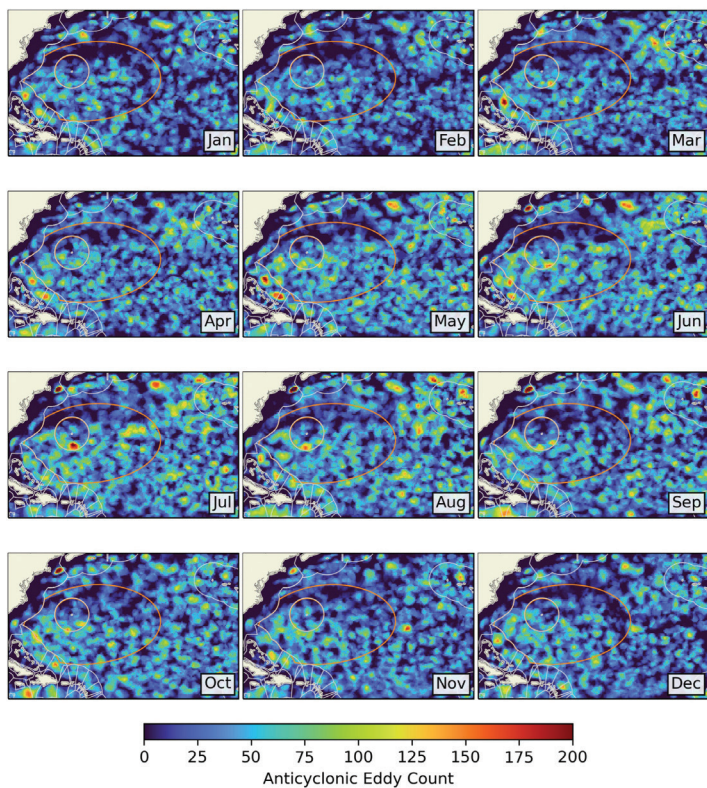
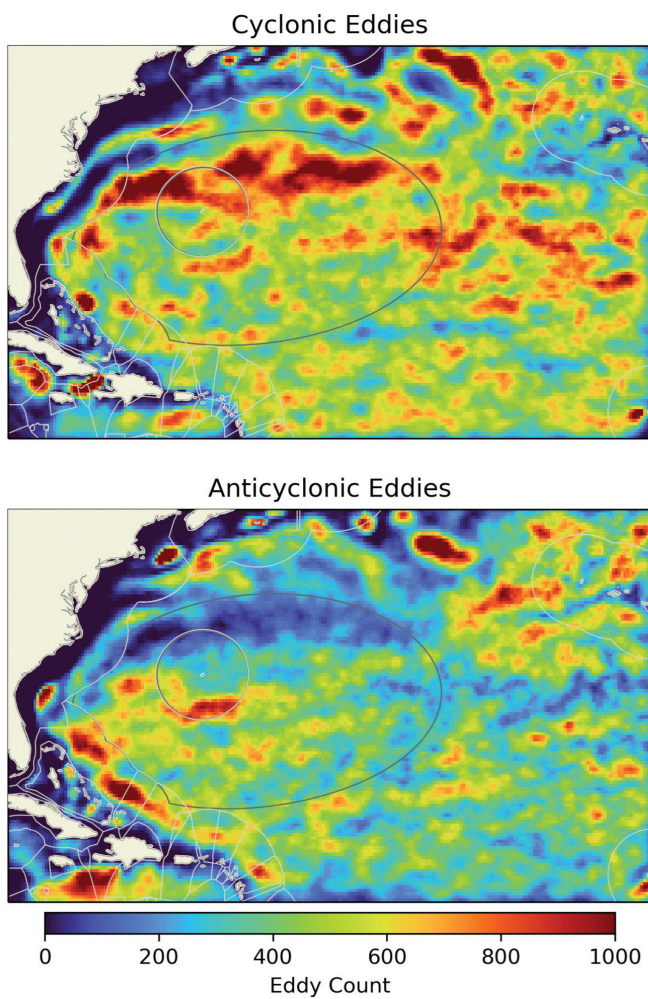


**FIGURE 10.** Monthly anticyclonic eddy count for the Sargasso Sea region for each month of the year.

**FIGURE 11.** Anticyclonic (lower) and eddy (upper) eddy count for the Sargasso Sea region over the complete study period.



dynamic topography. Sea level anomaly is the height of water over the mean sea surface in a given time and region whereas mean dynamic topography is the difference between the time-averaged sea surface and the geoid. This project used ADT data from the Copernicus Marine Environment Monitoring Service (CMEMS) (Table 1). This dataset provides gridded daily global estimates of sea

level anomaly based on satellite altimetry measurements and provides sea level anomaly data calculated with respect to a twenty-year mean reference period (1993-2012) using up-to-date altimeter standards (Taburet et al., 2019). We used these data to calculate monthly mean ADT (Figure 13) as well as an overall mean for the study period (Figure 12).

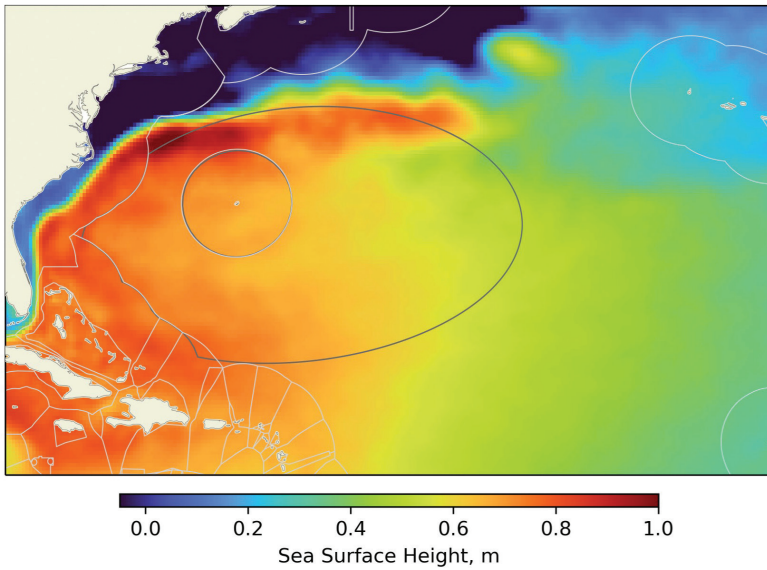


**FIGURE 12.** Mean absolute dynamic topography over the study period.

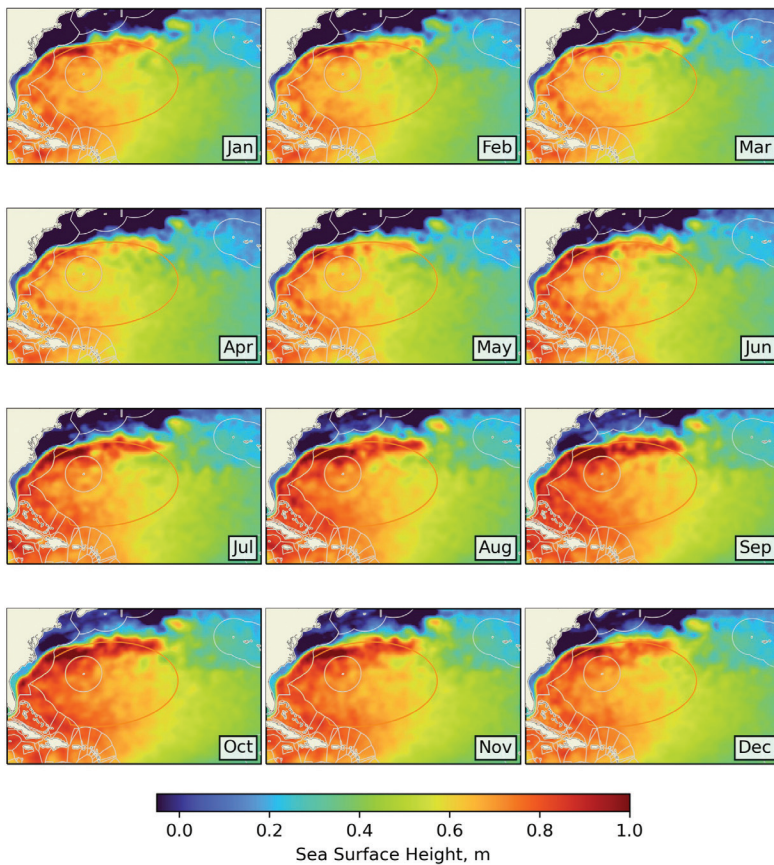


**FIGURE 13.** Mean monthly absolute dynamic topography.

### Salinity

Sea water salinity impacts life cycles of the fauna found in the Sargasso Sea, with potential implications for the reproductive success of some of the more sensitive species that occupy the region (Politis et al., 2021). This project used salinity data from the Hybrid Coordinate Ocean Model (HYCOM) (Table 1), which is part of the U.S. Global Ocean Data Assimilation Experiment (GODAE) (Cummings and Smedstad, 2013). HYCOM is

a data-assimilative hybrid isopycnal-sigma-pressure (generalized) coordinate ocean model containing variables (such as salinity and temperature) that have been interpolated between 80.48°S and 80.48°N. These data are logged at a 3-hour time interval, with eight data points per day of the month. We calculated mean salinity (psu) for the study period (Figure 14) as well as monthly mean climatology (Figure 15).

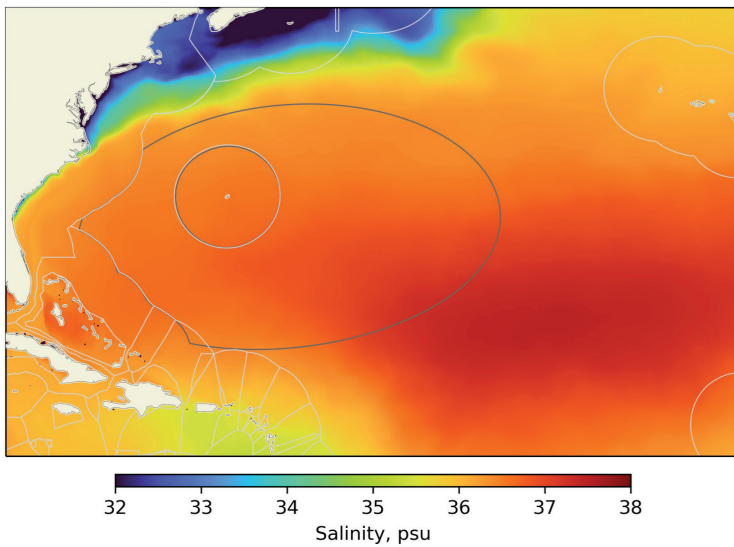


**FIGURE 14.** Mean salinity for the entire study period.

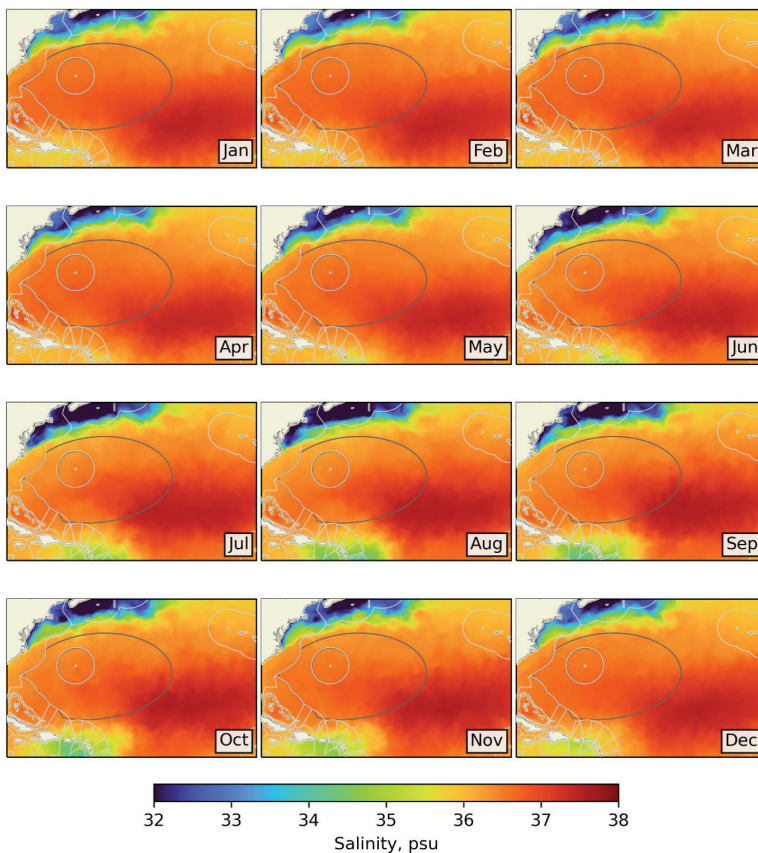


**FIGURE 15.** Mean monthly salinity.

### Chlorophyll-A Concentration

The concentration of chlorophyll acts as an indicator for biomass of phytoplankton in the water column, allowing inferences about primary productivity and related trophic dynamics in the study area. This project used chlorophyll-a concentration data from the Moderate Resolution Imaging Spectroradiometer (MODIS) dataset (Table 1; NASA, 2014). Near-surface concentration of

chlorophyll-a (chlor\_a) in  $\text{mg}/\text{m}^3$  is calculated using an empirical relationship derived from in situ measurements of chlor-a and blue-to-green band ratios of in situ remote sensing reflectances ( $R_{rs}$ ) (NASA, 2014). Data are provided as monthly concentrations for both yearly and 10-year means. Overall mean chlorophyll-a concentration was calculated for the study period (Figure 16) as well as monthly mean climatologies (Figure 17).

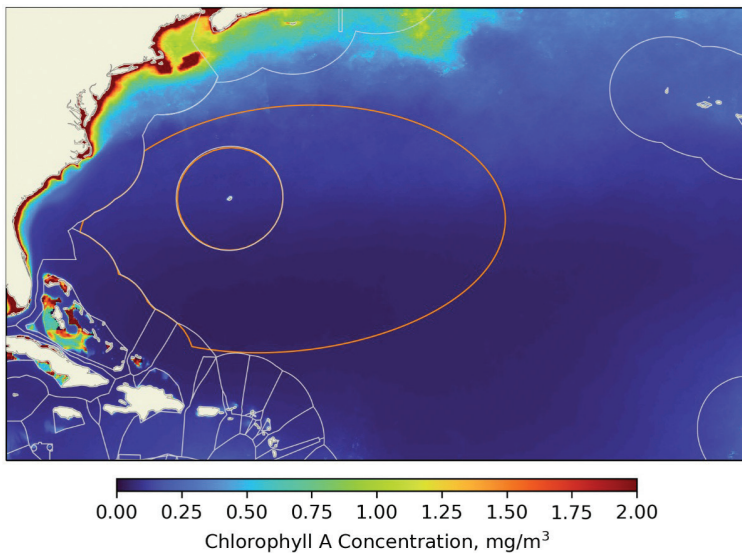


**FIGURE 16.** Mean chlorophyll-a concentration across the study period.

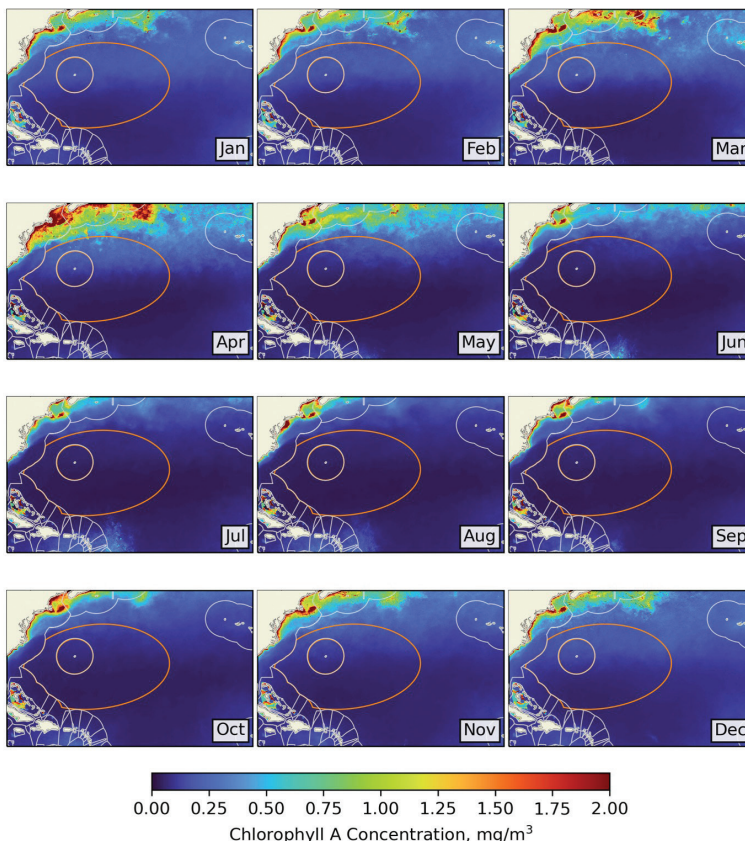


**FIGURE 17.** Mean monthly chlorophyll-a concentration.

## Ocean Water Temperature

### Surface Temperature

Although past reports on the delineation of the Sargasso Sea have found sea surface temperature (SST) to be too variable for identifying sub-regions of the feature (Ardron et al., 2011), we considered this variable important to include given its significance for certain biological communities (Miller et al., 2019). We therefore summarized sea surface temperature data as a parallel to our sub-

region analysis, the final version of which did not include incorporation of this variable. Sea surface temperature data was sourced from the Group for High Resolution Sea Surface Temperature (GHRSSST) surface temperature analysis, a version 4 Multiscale Ultrahigh Resolution (MUR) L4 analysis from several instruments on the NASA Aqua and Terra platforms (Table 1; JPL MUR MEaSUREs Project, 2015). Summarizations included overall mean temperature for the study period (Figure 18) as well as monthly mean sea surface temperature (Figure 19).

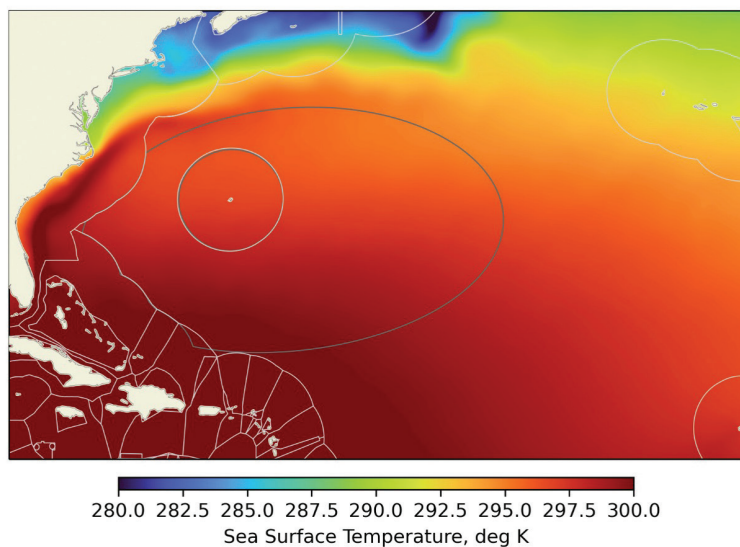


**FIGURE 18.** Mean sea surface temperature across the study period.

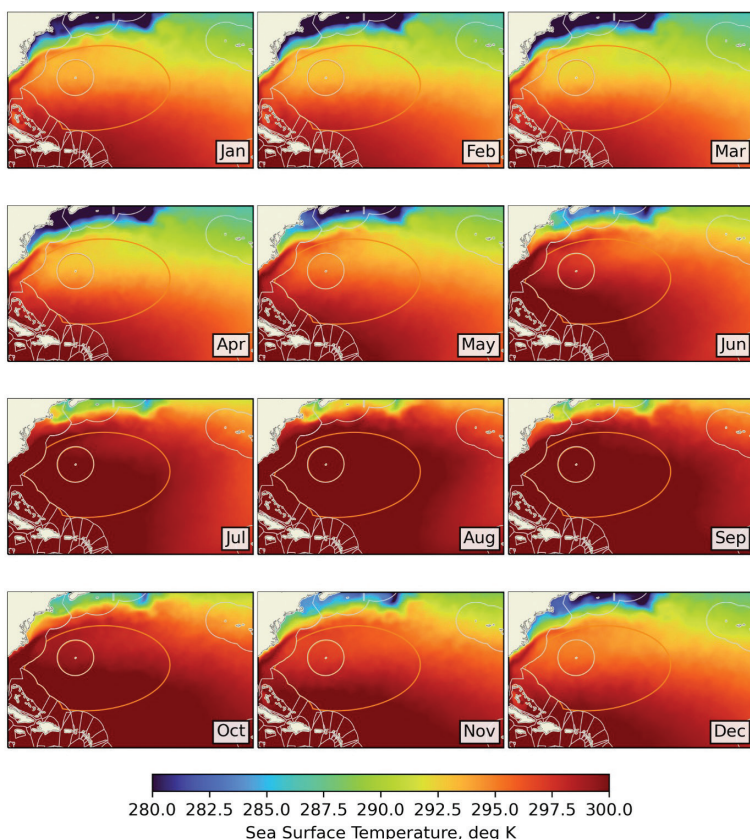


**FIGURE 19.** Mean monthly sea surface temperature.

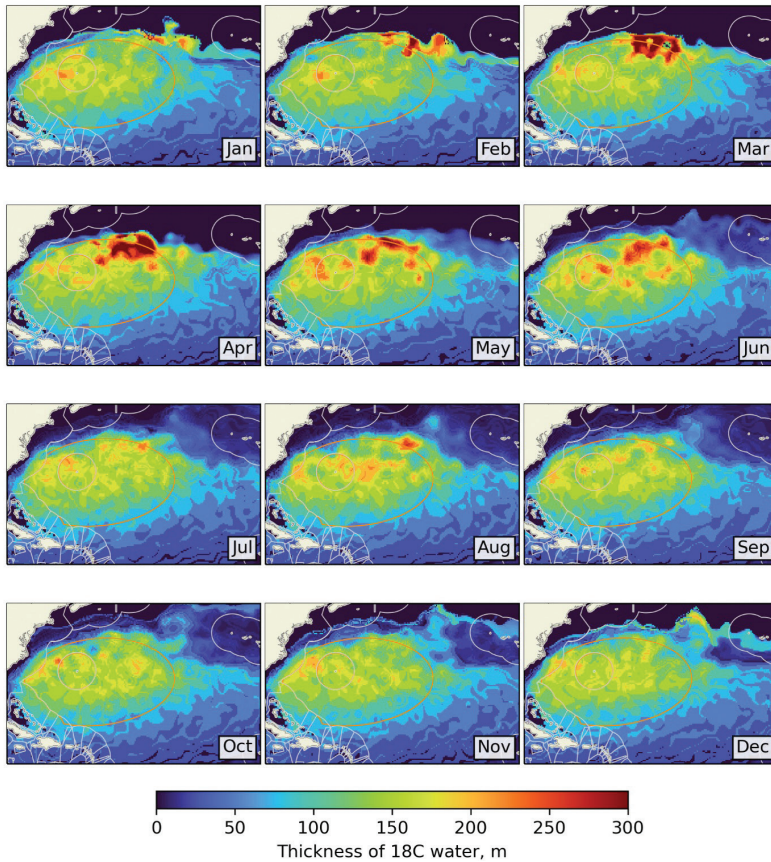


**FIGURE 20.** Monthly thickness of Subtropical Mode Water in the Sargasso Sea defined as water with a temperature between 17.5°C and 18.5 °C.

### **Subtropical Mode Water**

Subtropical Mode Water (STMW), which is also referred to as “18-degree water” is defined as a somewhat stable water mass with relatively homogenous temperature and density. STMW forms in the northern extent of the Sargasso Sea as intense cooling of the surface layer in the winter months causes deep mixed layers with temperatures of ~18°C that extend from depths of ~150m to ~400m (Lomas et al., 2011). At the onset of Spring, the STMW of the Sargasso Sea becomes capped by the seasonal thermocline and subducts to the south. Entrainment of the mixed layer during the winter months and subsequent influence on underlying STMW is a useful metric for evaluating seasonality as well as inter-annual variability in the area (Lomas et al., 2011). We included assessment of STMW water here (in parallel to our sub-region analysis) by determining thickness of this layer from month to month. For the purposes of this report, we defined STMW as water between 17.5°C and 18.5°C to allow for a slight temperature gradient that naturally occurs in this generally isothermal layer. For this analysis we use data from the World Ocean Atlas (Table 1) which is a collection of objectively analyzed, quality-controlled

temperature, salinity, oxygen, phosphate, silicate, and nitrate means based on profile data from the World Ocean Database (WOD). These data are available at a monthly time step as 0.25° gridded spatial resolution. We determined thickness of the STMW layer by calculating the difference between the depth to the 18.5°C water and the depth to the 17.5°C water, showing the thickness in meters of the layer of water within this temperature range. Figure 20 shows a monthly climatology of STMW within the study region.

### **Sea Surface Temperature Front Detection**

Sea-surface temperature fronts are areas where high horizontal temperature gradients are observed, occurring at various temporal and spatial scales (Cornillon 2007; Belkin *et al.* 2009). SST fronts are associated with ocean currents and upwelling and, as a result, tend to be more productive due to the increased supply of nutrients (Mahadevan, 2014). Here, we used the version 4 Multi-scale Ultrahigh Resolution (MUR) SST dataset described above. These data were analyzed using the Marine Geospatial Ecology Tools (MGET, Roberts et al., 2010) Cayula Cornillon Fronts tool, which implements Cayula

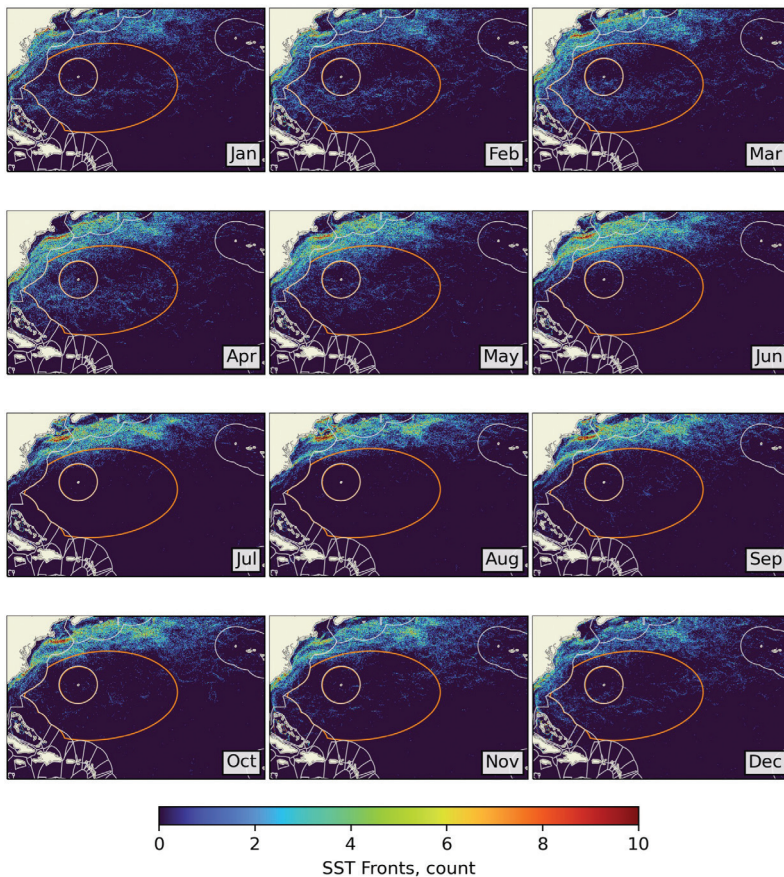


**FIGURE 21.** Monthly sea surface temperature front count.

and Cornillon's (1992) single image edge detection algorithm to identify sea surface temperature fronts. Fronts were summarized as a monthly climatology wherein front count was grouped by month across the entire study period (Figure 21).

### Seascape Pelagic Habitat

Seascape Pelagic Habitats are a method for characterization of the 4-dimensional variability of dynamic marine pelagic ecosystems using improved classification methods, remote sensing products, advances in autonomous sample of biological complexity, and observational networks (Kavanaugh et al., 2016). The US and global Marine Biodiversity Observation Network (MBON) partnered with the US Integrated Ocean Observation System (IOOS), NOAA/OAR/AOML and NOAA/NESDIS/STAR to develop and routinely generate this Seascape Pelagic Habitat Classification product (MBON Seascapes). These seascapes provide information about the extent and quality of different pelagic habitats, identifying spatially explicit water masses with particular biogeochemical features, and can be used to assess planktonic and fisheries communities that reside therein. There

are 33 total Seascape Pelagic Habitat classes, all with a distinct combination of environmental and oceanographic variables. Current MBON Seascapes products include monthly and 8-day time steps at 5 km resolution.

Our analysis implemented the monthly MBON seascape data product, which we used to calculate the monthly mode of seascapes over the study period (Figure 22) to find the classes most frequently represented across the study area (Table 2).

### Ecological Marine Units (EMUs)

The Ecological Marine Units (EMUs) classification is a data-derived ecosystem mapping approach containing 37 distinct 3-dimensional volumetric regions of ocean properties most likely to drive ecosystem responses (Wright et al., 2018). This dataset consists of a global point mesh framework wherein each point carries values for six different chemical and physical oceanographic structure attributes: temperature, salinity, dissolved oxygen, nitrate, silicate, and phosphate. While we mapped EMUs in the study region, this variable was not particularly helpful in describing the feature, with only very broad discernable patterns in space and time. We therefore decided against

**TABLE 2.** Seascape pelagic habitat classes represented in the study area and corresponding descriptions.

Seascape ID Number	Nominal Descriptor	SST (*C)	SSS (psu)	ADT (m)	ICE (%)	CDOM (m <sup>-1</sup> )	CHLA (mg/m <sup>2</sup> )	NFLH (W m <sup>-2</sup> um <sup>-1</sup> sr <sup>-1</sup> )	NFL-H:CHL	Latitude	Dominant Hemisphere	Dominant Season
3	Tropical Subtropical Transition	24.12	35.34	0.68	0	0.01	0.15	0.06	0.4	Tropical	Both	Year Round
5	Subtropical Gyre Transition	23.95	35.89	0.71	0	0	0.07	0.04	0.5	Subtropical Temperate	Both	Autumn-Winter
7	Temperature Transition	12.98	34.72	0.37	0	0.01	0.28	0.11	0.41	Temperate	Both	Winter
11	Tropical/Subtropical Upwelling	22.94	34.79	0.883	0	0.01	0.27	0.11	0.39	Tropical, subtropical	Both	Winter
13	Subtropical Gyre Mesoscale Influenced	23.47	35.89	0.52	0	0.01	0.1	0.02	0.19	Subtropical Temperate	Both	Spring-Summer
14	Temperate Blooms Upwelling	9.95	33.91	-0.01	0	0.03	0.84	0.16	0.19	Temperate/Subpolar	Both	Spring-Summer
15	Tropical Seas	25.35	35.4	0.51	0	0.02	0.32	0.06	0.2	Tropical/Subtropical	Both	Wintr
17	Subtropical Transition Low Nutrient Stress	20.89	33.59	0.64	0	0.01	0.17	0.02	0.15	Tropical/Subtropical	North	Summer
20	Subtropical, Fresh Influenced Coastal	27.45	31.82	0.88	0	0.02	0.34	0.06	0.18	Subtropical	North	Winter/Year-Round
21	Warm, Blooms, High Nuts	22.54	34.46	0.57	0	0.07	2.09	0.24	0.12	Tropical/Subtropical	Both	Winter/Year-Round

including this variable in our final feature description and classification process.

### Sargassum Seaweed Detection

The detection of Sargassum is vital to understanding the movement of this feature in space and time. Several methodologies implementing remote sensing products have been developed to identify floating algae, including Sargassum. These datasets are derived from various algorithms run on data from a variety of remote sensing platforms (MODIS, VIIRS, Sentinel 3, and GOES). Here, we explored implementation of the Floating Algae Index (FAI) and Alternative Floating Algae Index (AFAI) (MODIS derived), as well as the Maximum Chlorophyll Index (MCI; Sentinel derived). While we were able to implement these data products to detect *Sargassum* within a certain spatial extent and found the MCI to be particularly illuminating in the context of this report, spatial coverage

of these products does not extend across the entire study area. Due to the limited coverage, which generally only extended across the southernmost third of the study area, we were unable to incorporate this variable in our sub-region classification process and decided against including results from these data exploration into the final feature description. However, we hope to explore these resources in more depth to prepare a summarization and analysis as part of Deliverable 3 of this project (analyze and synthesize existing research and information: ecosystem state evaluation).

### Sub-Region Detection

#### Summary Statistics

As an initial step for our sub-region analysis, we calculated summary statistics for each of the environmental variables listed above using the preliminary sub-regions

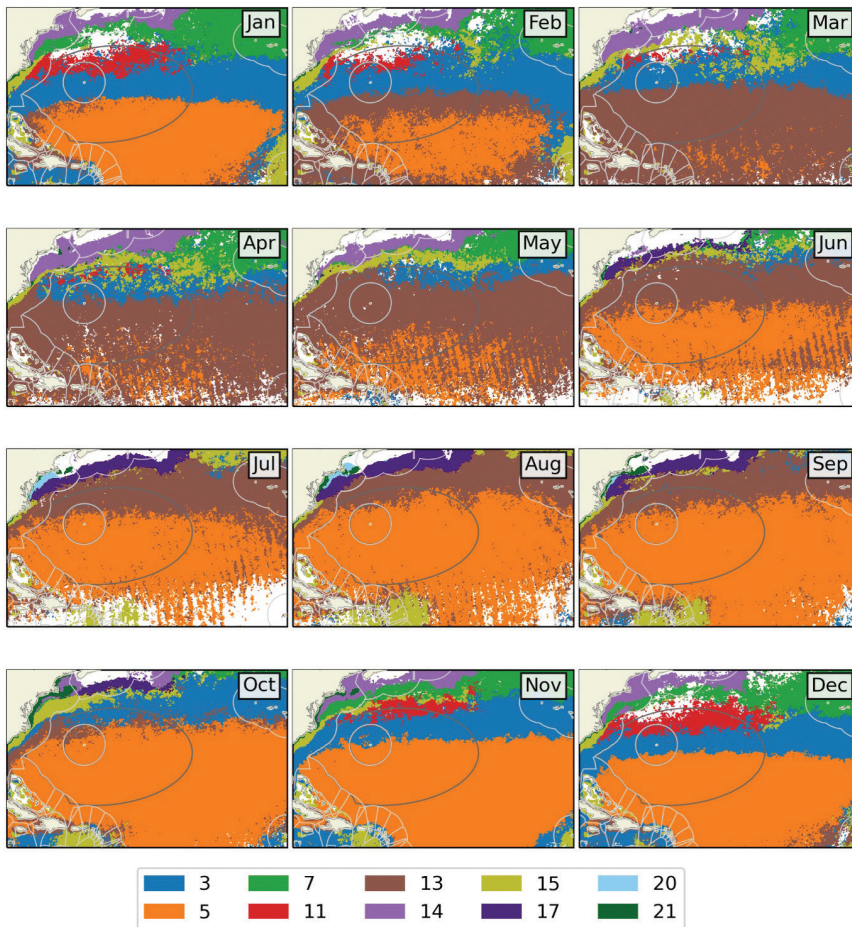
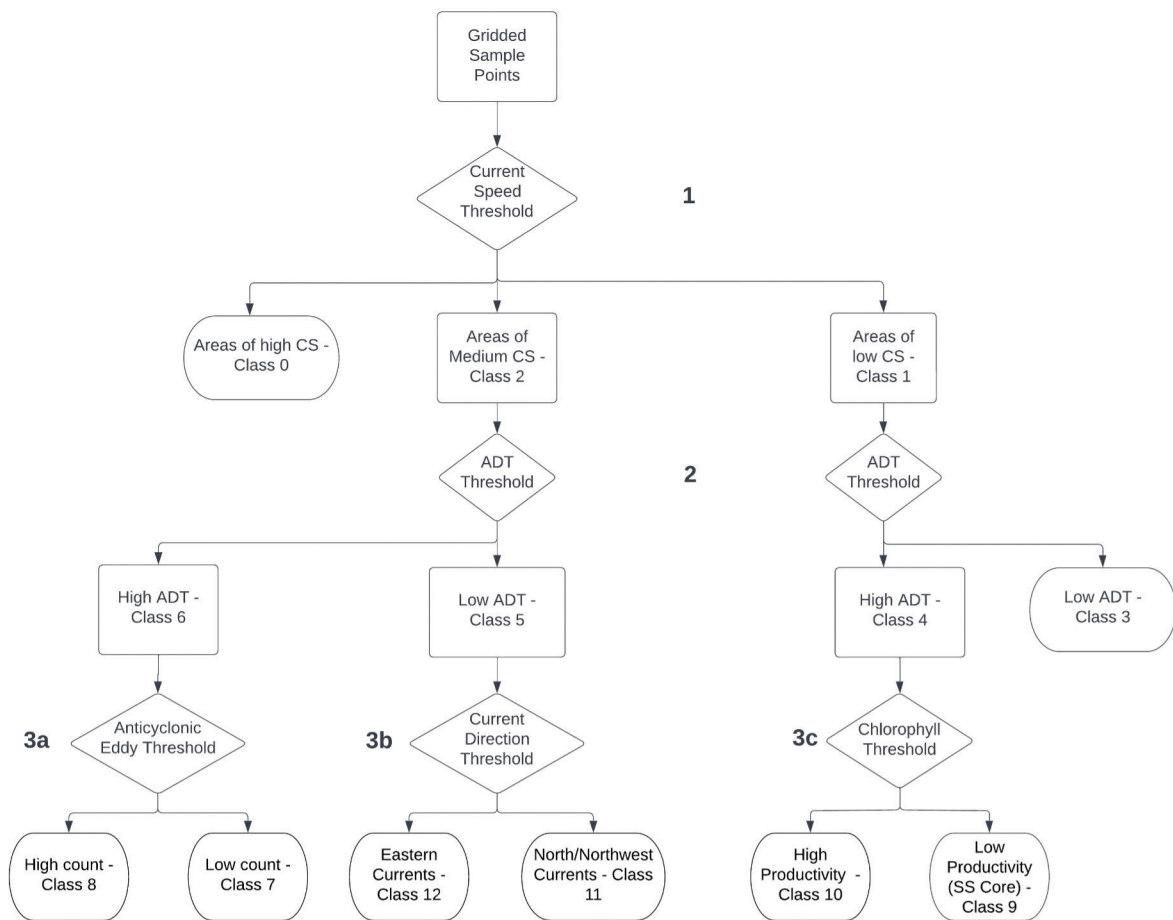


**FIGURE 22.** Monthly mode of seascape pelagic habitats for the study region

(PSR) produced by the 2011 work (see above, Ardron et al., 2011). Firstly, we generated a .09° (approximately 10 km) regular grid of geo-referenced sample points which we used to extract values from raster data for each of the environmental variables. The resulting data frame included spatially referenced gridded points throughout the study region with an associated value, both overall and per month, for each variable including eddy count (anticyclonic), absolute dynamic topography (m), chlorophyll-a concentration (mg/m<sup>2</sup>), current speed (m/s), current direction (°) sea surface temperature (°C), and salinity (psu). We identified which PSR each point belonged to (Gulf Stream, Azores Current, Equatorial Current, Antilles Current, Sargasso Sea – Core, and Sargasso Sea – Gulf Stream transition) and included this information as an attribute. Finally, we produced summary statistics for each PSR by grouping points according to their sub-region attribute and calculating values for minimum, mean, standard deviation, maximum and median for each environmental variable. We did this for each month of the year as well as the overall study period.

### K-Means Analysis

K-means clustering is an unsupervised classification method for identifying groups or clusters of data points based on similarities in their multidimensional environmental characteristics. This process requires the input of a set number of clusters ( $k$ ) which the K-means algorithm uses to group data points. The algorithm iteratively identifies the pre-determined  $k$  number of centroids and then assigns every data point to the nearest cluster while keeping the centroid as compact as possible. In this analysis the number of clusters ( $k$ ) was determined through a sensitivity analysis of spatial trends in the above environmental variables within the study region. We used the overall summarizations of environmental data for training data, which determines centroids and attributes of each of the clusters, and the monthly climatologies to test the distribution of these clusters. Although we had some success in sub-region delineation as defined by k-means clusters, ultimately, we decided to forgo this unsupervised method for an alternative supervised one, allowing for the implementation of informed decision rules.



Decision Rule	Variable	Number of Resulting Groups	Threshold value(s)
1	Current Speed (m/s)	3	Greater than 0.2; Less than 0.2 & greater than .05; Less than 0.05
2	Absolute Dynamic Topography (m)	4	Greater or less than 0.6
3a	Anticyclonic Eddy (count)	2	Monthly: greater or less than 40; Overall: greater or less than 250
3b	Current Direction (°)	2	Greater than 270 (heading northwest) or between 45 and 135 (heading northeast/southeast)
3c	Chlorophyll-a Concentration (mg/m <sup>3</sup> )	2	Greater or less than 0.05

**FIGURE 23.** Decision tree classification matrix including decision rule criteria for each variable.

### Supervised Decision Tree

The supervised decision tree is a method of classifying features that allows for informed decision rules based on values of the features themselves, allowing us to implement pre-existing knowledge of the region and its ecology into the classification process. Using summary statistics (described above) as a starting point, we evaluated major differences in environmental variable values

between areas within the study region. For example, there are noticeable divisions in current speed values that split the study region into three primary areas: those of relatively high current speed (the Gulf Stream), those of medium current speed (the peripheral currents to the southeast and southwest) and those of low current speed (the center of the Gyre) (Figure 23, 1). We used current speed as the first decision rule for categorizing the region,

with threshold values show in Figure 23. In addition to allowing for informed decision rules, the supervised decision tree also allowed us to suspend classification when the area in question was not of particular importance and therefore didn't require further sub-division. Thus, once the Gulf stream sub-region was categorized by the first decision rule, it was not subject to any additional decision rules (Figure 23). The second round of decision rules were centered around ADT, with areas of medium current speed and low current speed split by the same ADT threshold criteria (Figure 23, 2). Current speed and ADT both provide insight into the amount of energy in a system, and the incorporation of these two variables into the initial decision rules allowed us to sub-divide the region in a way that reflects partitioning naturally created by energy from the currents and gyres in and around the Sargasso Sea.

We continued classification of three of classes four, five and six by three different decision rules including criteria based on anticyclonic eddy count, current direction, and chlorophyll-a concentration, respectively (Figure 23; 3a, 3b, and 3c). Class four was sub-divided by the chlorophyll-a concentration decision rule, isolating areas of the Sargasso Sea core with higher and lower productivity. Class five was split further by a current direction threshold in order to identify the weaker bounding currents that occur to southeast and southwest. Finally, class six was sub-divided by an eddy count decision rule to isolate the medium energy area to the immediate south of the Gulf Stream and the lower energy area to the southwest of the study region. Due to the difference in timespan between the monthly climatologies and overall mean data summarizations, with eddy counts for any single month significantly lower than across and 12 months of the year, the decision rule threshold value for anticyclonic eddy count in the monthly climatology classification was different to that of the overall classification (Figure 23) to adjust for this discrepancy.

While categorized sample points displayed noticeable zonal trends (Figure 24), we determined that the amount of noise observed in this product might prove to be problematic for further data summarizations and management initiatives. We therefore performed two generalizing steps in ArcGIS Pro to reduce noise in the final sub-region layer. Categorized points were imported into ArcGIS, converted to a raster data layer, and then run through a focal statics tool and a boundary cleaning tool, both of which are part of the Spatial Analyst toolbox developed by ESRI (<https://pro.arcgis.com/en/pro-app/>

[latest/tool-reference/spatial-analyst/an-overview-of-the-spatial-analyst-toolbox.htm](https://pro.arcgis.com/en/pro-app/latest/tool-reference/spatial-analyst/an-overview-of-the-spatial-analyst-toolbox.htm)). The focal statistics tool calculates for each input cell location a statistic of the values within a specified neighborhood (<https://pro.arcgis.com/en/pro-app/latest/tool-reference/spatial-analyst/focal-statistics.htm>). Our analysis used a circular neighborhood with a seven-cell radius, identifying the majority value (value that occurs most often) of the cells in the neighborhood. We used the boundary cleaning tool on the focal statistics results raster to smooth boundaries between zones. This tool was set to use a descending sort type, wherein raster zones are sorted in descending order by size. Those with larger total areas have a higher priority to expand into ones with smaller total areas which helps to eliminate or reduce the prevalence of cells from smaller zones in the smoothed output. The product of the boundary cleaning process was the final version of the sub-region delineation, with each of the classes included in the final raster data representing a unique combination of environmental variables as defined by the supervised decision tree classification.

The final step of the decision tree classification was to evaluate regions of stability based on categorization. Stability reflects areas that are categorized as the same class for an extended period which we determined by taking the mode of the 12 monthly categorized rasters. The mode indicates which class is represented most frequently throughout the 12 months of the year. Additionally, we included in our analysis the mode count, which is the number of months the mode occurs throughout the year. Thus, stability within a given area of the study region directly relates to increasing mode count, with 12 being the most stable corresponding to those areas that are categorized as the same class throughout the entire year.

## Results

The supervised decision tree ultimately produced 9 distinct classes with varying ecological characteristics (Table 3). Figure 24 (bottom) shows the distribution of each class throughout the study area based on categorization of gridded points with corresponding environmental variable values that represent summarizations for the entire study period (see above, methods section). The predominant classes represented within the previously delineated Sargasso Sea Alliance Study Area (hereafter Study Area) are 3, 7, 9, 10 (Figure 24). Class 0, which was defined during the first round of decision rules as an area of high current speed, aptly corresponds with the Gulf

**TABLE 3.** Description of each sub-region class as defined by the supervised decision tree classification

Class Number	Characteristics	Description
0	High current speed	Gulf Stream zone
3	Low current speed, low ADT	Low energy zone
7	Medium current speed, high ADT, low anticyclonic eddy count	Transition zone
8	Medium current speed, high ADT, high anticyclonic eddy count	Antilles Current and margins
9	Low current speed, high ADT, low productivity	Lower productivity core
10	Low current speed, high ADT, high productivity	High Productivity core
11	Medium current speed, low ADT, north/northwest current direction	North Equatorial Current zone
12	Medium current speed, low ADT, eastern current direction	Azores Current zone

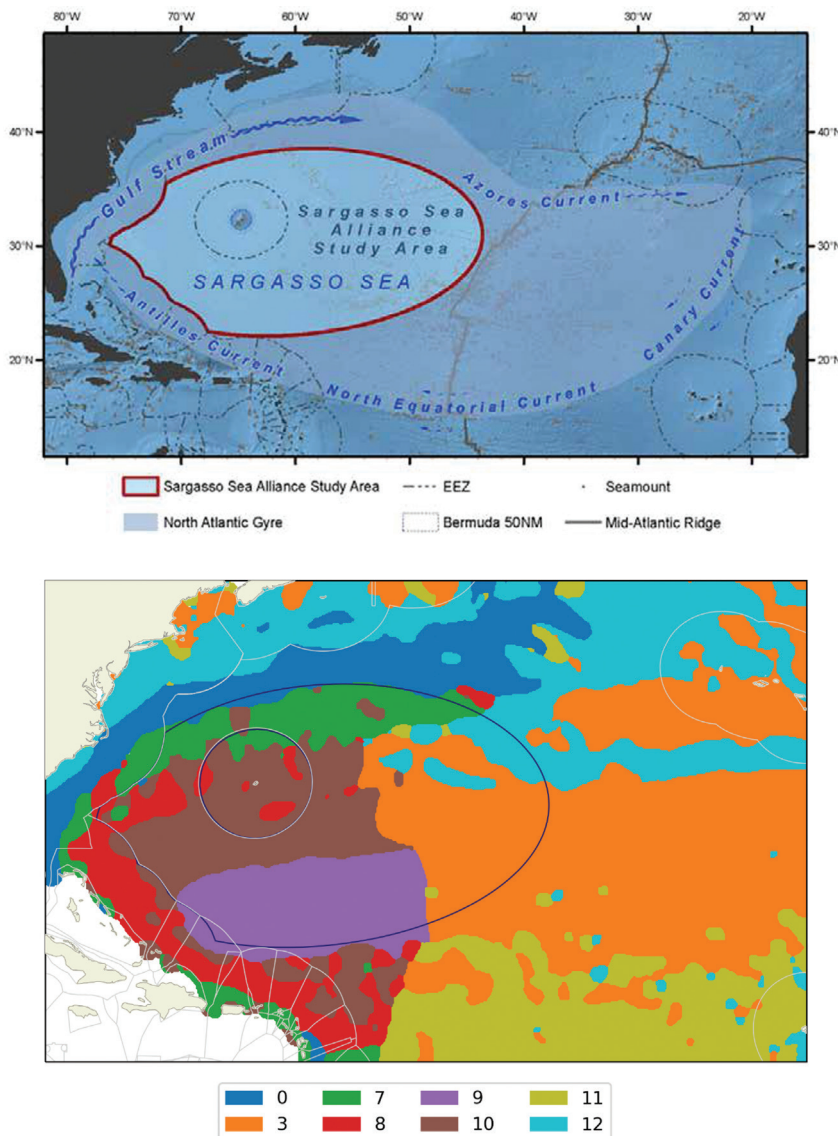


**FIGURE 24.** Major currents relative to the Geographical Area of Collaboration (top) and decision tree classification of the study area (bottom).

Stream, and can be seen closely bounding the northernmost margin of the Study Area. Similarly, Class 8 runs along the southeastern edge of the Study Area, reflecting the presence of the slightly lower energy Antilles Current and its margins.

Just south of the area predominantly covered by Class 0 there is a section dominated by class 7, representing a transition zone between the high energy region in and around the Gulf Stream, and the lower energy area at the center of the Study Area (Figure 24). Bounded by classes 8 and 7 is the region at the center of the Study Area which is split between classes 9 and 10. These classes represent the low energy center of the Study Area and the greater North Atlantic Gyre where sargassum mats aggregate. Classes 9 and 10 differ in the level of primary productivity, with class 10 characterized as the more productive of the two (Table 3).

Along the eastern margins of the Study Area, three predominant classes are represented: 3, 11, and 12. Class 3 is not only characterized by low current speed (similar to the Core classes) but also low ADT and thus represents the lowest energy class within the region. Classes

11 and 12 are areas of higher energy that differ only by current direction, with class 11 corresponding to north/northwest flowing North Equatorial current area and 12 corresponding with the eastern flowing Azores current.

Figure 25 shows the classification criteria outlined above applied to the gridded sample points with corresponding environmental variable values that represent summarization by month (see above, methods section). These plots reveal the seasonality of the core Study Area, with Class 10 (high productivity core) expanding during the colder months (November, December, January, February) as chlorophyll-a concentrations rise, and contracting during the warmer months (June, July, August, September) as productivity decreases. During the months of September, October and November, the transition zone (Class 7) expands into the Core area. Partly defined as an area of medium current speed, the increase in coverage by Class 7 into areas generally covered by a combination of classes 3 and 10, indicates more widespread areas of “medium” current direction just beneath the Gulf Stream zone.

While the Antilles current and margins (Class 8) is

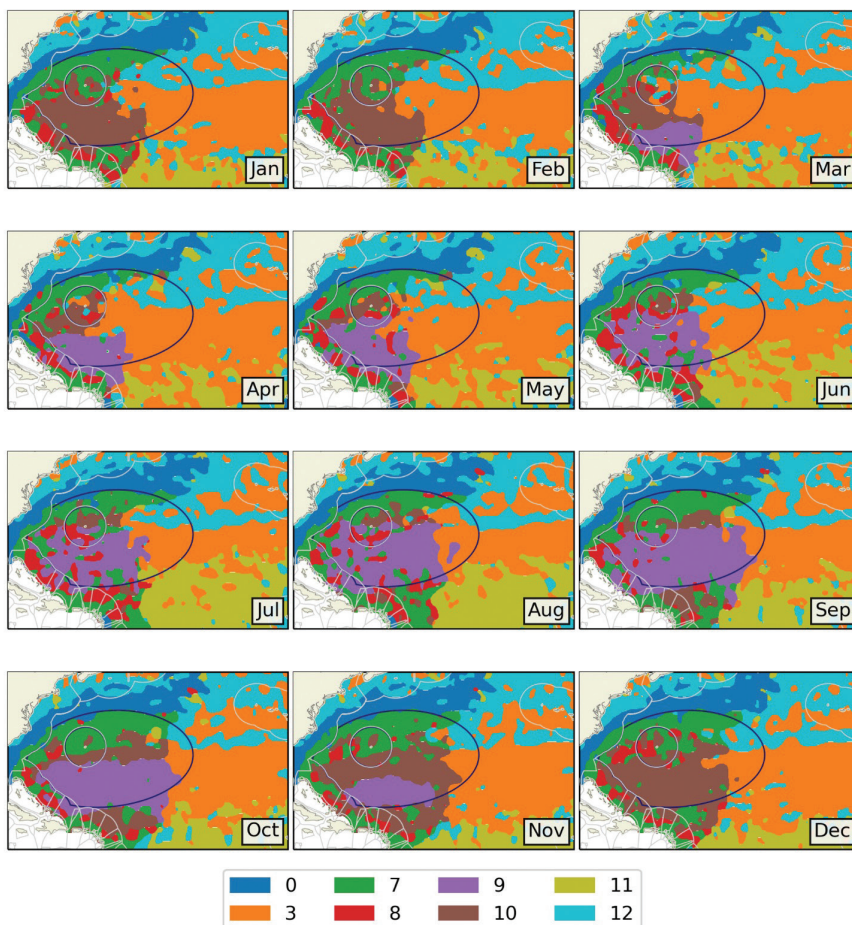


**FIGURE 25.** Monthly decision tree classification of the study region.

discernable in the overall point classification layer (Figure 24, lower), it is less so in the monthly climatology classification. Despite becoming more prominent during the months of May, June and July, Class 8 remains patchy throughout the year. This might be attributed to the fact that the Antilles current notably appears as more of an eddy field along the Bahamas-Antilles arc rather than as a continuous jet (Gunn and Watts, 1982), accounting for isolated areas of higher eddy count and thus characterization into Class 8.

Between June and December, coverage of the low energy zone (Class 3) contracts eastward, relinquishing area to the Core Classes (9 and 10) and the Transition Zone class (Class 7). Consistent through the year, however, is the connection between the Study Area and Class

12, the Azores Current zone, which stretches out from the core area east across the Atlantic. Finally, Class 11 (Northern Equatorial zone) becomes patchy and contracts intermittently throughout the year, potentially owing to the influence of the weaker and more meandering North Equatorial Counter Current (NECC). Given that Class 11 is partly defined by current direction (North/Northwest), it would follow that, under the influence of the less easily categorized NECC, areas of Class 12 (defined by an eastern current direction) would occur in patches as this current system becomes more prominent.

Figure 26 shows the mode and mode frequency of classified areas throughout the year, with the top map indicating the class that is most frequently represented in each pixel over the 12 months. This method is useful in

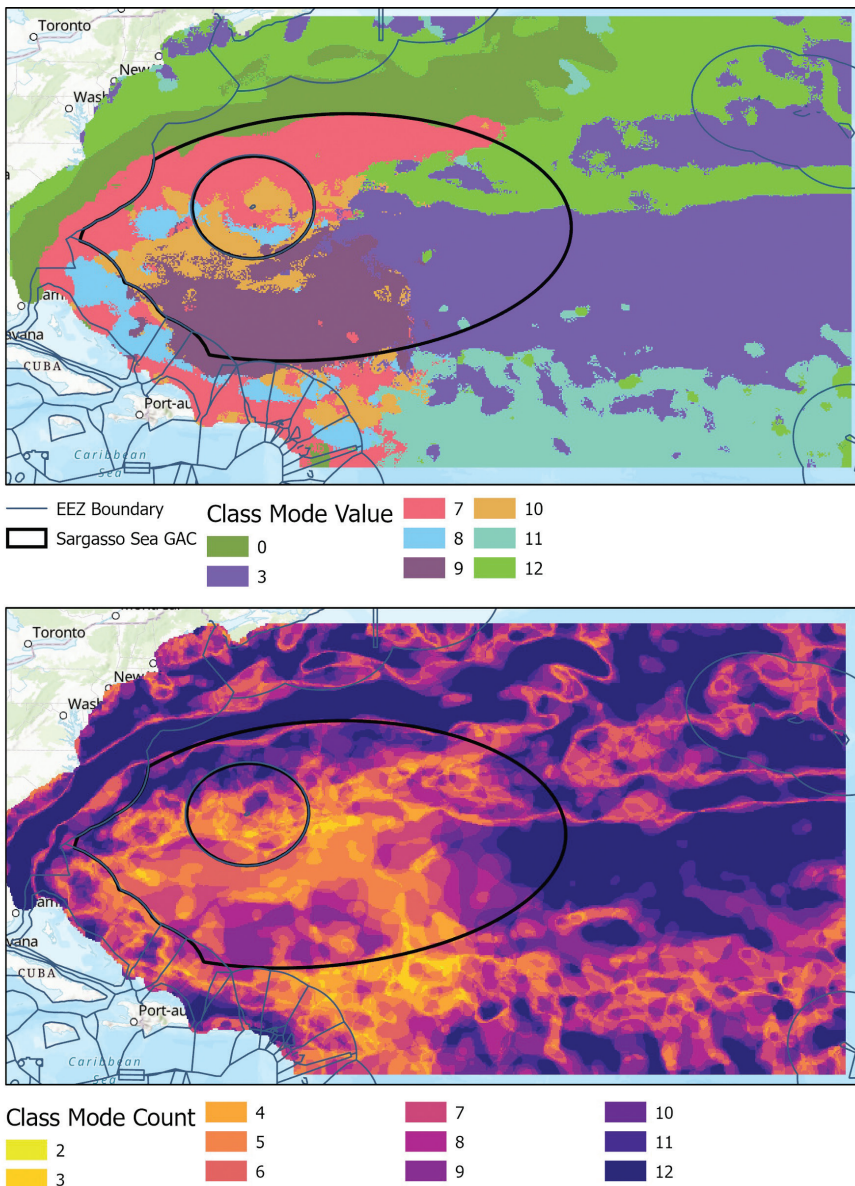


**FIGURE 26.** Mode class of monthly decision tree classification (above) and mode frequency (below). Areas with a higher mode frequency, or count, reflect those of increased stability throughout the year and lower seasonal variation.

determining stability of the study area, with the frequency (or count) of the mode showing how many months the predominant class occurs, ranging from 2-12. Areas with higher mode count, those represented in cool colors in the bottom map of Figure 26, are relatively stable areas with regards to our classification method and seldom or never change in categorization from month to month. Conversely, areas symbolized by warmer colors represent those where the mode frequency is low with the dominant class occurring during fewer than half of the months in the year.

The more stable areas appear to correspond to the Gulf Stream and its margins, the area just south of the Azores current, and the southwest margins of the study area. The core of the Sargasso Sea ellipse, however, appears more variable in nature, reflecting seasonal changes in the monthly categorization shown in Figure 25. It is worth noting, however, that within the core area there is slight differentiation between the area south of the Gulf Stream margins (the area around Bermuda, categorized by mode count values of 4-5 and below) and the southernmost area of the ellipse (with mode counts between 8-9), with higher stability seen to the south (mode class 9) as compared to the Transition zone further north (mode classes 7, 9, 10 and 11).

Our classification methodology offers useful insight into existing spatio-temporal trends in the behavior of the Sargasso Sea. Sub-regions revealed by spatial distribution patterns of these classes are potentially valuable in the next steps of this project, which is to summarize biological and human use activity in and around the Sargasso Sea. We therefore anticipate further aggregation of these classes into more centralized sub-regions that reflect the general ecological, temporal and spatial trends that results from our classification have revealed. Ultimately, we hope to develop sub-region boundaries that will enable the summarization of human use and biological data with more specific spatial aggregations in mind. In this way we will be able to synthesize the work performed in this phase of project with these next steps, creating linkages between trends revealed by this classification, biological use, and human activity.

## Discussion and Conclusion

The summarization and synthesis of various oceanographic variables conducted in this report reveal a useful methodology for an in-depth examination of the Sargasso Sea and its dynamic nature in space and time.

With the incorporation of several key oceanographic variables and implementation of the supervised classification method described above, our analysis has synthesized existing knowledge pertaining to factors that influence the behavior of this feature. While there are limitations to the methodology and the results we've outlined here, this work is a promising beginning to proceeding work focused on synthesizing human use and biological data.

Past analyses focused on identifying the Sargasso Sea in space and time have highlighted several variables of particular interest, including signals from SST and STMW, in possible sub-division of this feature into biogeographic regions (Ardron et al., 2011). While results from SST summarizations from this project reveal a largely predictable seasonality to the study area, behavior of STMW appears to be a useful jumping off point for the examination of the Sargasso Sea and its spatial dynamics. Our results indicate that areas of mode water thickness of 100m and above correspond closely to the Sargasso Sea Geographical Area of Collaboration, and in this way might act as a preliminary signal for the presence of this feature. The incorporation of STMW also provides useful insight into the depth component of this feature, drawing the pelagic zone, which acts as vital representation for certain high conservation value species associated with the Sargasso Sea (Block et al., 2001; Loefer et al., 2007), into the descriptive process.

Also referenced in the 2011 report is the potential role of eddies in biogeographic region classification (Ardron et al., 2011). In this analysis, the incorporation of variables such as eddy count as well as current speed, absolute dynamic topography, and current direction help reveal areas of high and low energy, which are likely to impact distribution of *Sargassum* as well as biogeochemical processes in the upper ocean (Lomas et al., 2011). For example, *Sargassum* is transported from areas of growth in the Gulf of Mexico to the North Atlantic Gyre by a network of current systems and is further aggregated by eddies (Benitez-Nelson and McGillicuddy, 2008). To this end, the classification method outlined here might help illuminate areas where *Sargassum* is aggregated for longer periods of time as well as those where concentration is likely more intermittent. In areas that are less stable and/or categorized by high energy sub-classes (e.g. the area just south of the Gulf Stream), we might see lower aggregation of *Sargassum*, whereas those areas that are stable and categorized by low energy sub-classes (the area on the eastern fringe of the Geographical Area of Collaboration) might see a greater aggregation of mats

for a more prolonged period of time.

These elements come together to shed light on this highly complex feature, and how classification into sub-regions by incorporation of dynamic variables might capture the fluidity, variability, and seasonality of the Sargasso Sea in space and time. In fact, results from our sub-region classification suggest that potential adjustments to the Geographical Area of Collaboration might be useful in the effort to better encompass the Sargasso Sea in its entirety, such as inclusion of greater coverage in the eastern extent of the study region as well as to the south.

The process for descriptive analysis we have outlined here highlights the importance of improving understanding of the Sargasso Sea and its distribution in space and time using dynamic variables to inform effective management strategies. With continued refining, these methods might enable stakeholders to pinpoint areas of enhanced conservation interest, such as those where *Sargassum* habitat is more robust and therefore supports greater biodiversity or species abundance. However, it is important to note limitations of this study and potential implications for broader management initiatives including the role of this analysis in the future EDA.

Firstly, this report and the methodologies therein did not take into consideration the influence of larger climatic phenomena, namely the Northern Atlantic Oscillation (NAO) or the Atlantic Multi-Decadal Oscillation (AMO). The vast coverage of the Sargasso Sea study area means that potential impacts of these broader oceanographic phenomena might behave differently between different sub-regions. Examination of these impacts was determined to be outside the scope of our work and would require more in-depth input from experts in this field.

Second, the development of methods to examine the relationship between preliminary biogeographic regions described here and the presence of *Sargassum*, which is ultimately a defining factor of the ecology of the Sargasso Sea, will be an important next step. To do this, a more accurate detection of the presence of *Sargassum* over a longer time period is needed to provide context for the analyses summarized in this report. New algorithms for detecting *Sargassum* from satellites do exist, but these datasets do not yet provide adequate spatial and temporal coverage of the Sargasso Sea region, instead focusing on nearshore areas and the emergent Great Atlantic *Sargassum* Belt. Information pertaining to *Sargassum* distribution and abundance is needed, however, to more accurately examine how and to what

degree our methodology could play a role in accurately predicting the spatial and temporal distribution of the Sargasso Sea.

Third, owing to the generally complex nature of the Sargasso Sea, there are limits to the ability of these analyses to empirically determine the exact extent, in both space and time, of this feature from existing data. For example, results from many aspects of our analyses reveal a fluid feature boundary in the eastern extent of the study area. A good example of this can be observed our summarization of STMW, which shows a well-defined thick Mode Water layer in the western side of the Geographical Area of Collaboration that becomes steadily thinner towards the eastern side of the extent as it diffuses out over this lower energy area. This area is defined by sub-classes that are generally low energy in nature, with slow current speed and/or low ADT in all three of the classes that it is commonly categorized by (classes 3, 11, 12).

Furthermore, it is worth noting that results from our stability analysis indicate that certain areas of high variability exist within the study region, highlighting the transitional and seasonal nature of zones such as the Sargasso Sea core and southern boundary of the Geographical Area of Collaboration. The fluid nature of the eastern boundary of this feature as well as the relatively unstable zones identified in our sub-region analysis emphasize that assigning fixed boundaries in space for a feature that is noted for the fluidity, variability and seasonality of its constituent parts can never be exact or relied on too heavily. Results from our classification should therefore be implemented as a means to understand and quantify these characteristics, as well as provide context to human and biological use trends to highlight broader areas of interest, rather than acting as a hard-and-fast delineation of this feature in space and time.

This report is the first step of a multistage project to more fully understand the Sargasso Sea and results outlined here offer a jumping off point for promising next steps in this effort. Further analyses to build upon the foundation established by this report will include examination of ecosystem state, which will incorporate further exploration of *Sargassum* detection methodologies. An additional next step in linking sub-regions of the Sargasso Sea to biological data will include assessing use of the study area by high-conservation values species such as European and American eels, cetaceans, and turtle species.

This next phase will also explore several dimensions of human use, including the location and seasonality of

shipping traffic through the Sargasso Sea. This effort will also involve linking variables used here to climate predictions from several models in the Coupled Model Intercomparison Project Phase 6 (CMIP6) to assess how our methods might be used to understand behavior of this feature into the future. Possible future work could be to examine pollution within the Sargasso Sea study area, which is a central concern to conservation efforts due to the concentrating effect of the North Atlantic Gyre.

## Literature Cited

- Ardron, J., Halpin, P., Roberts, J., Cleary, J., Moffitt, M. and J. Donnelly 2011.** Where is the Sargasso Sea? A Report Submitted to the Sargasso Sea Alliance. Duke University Marine Geospatial Ecology Lab & Marine Conservation Institute. Sargasso Sea Alliance Science Report Series, No 2, 24 pp. ISBN 978-0-9847520-3-4
- Belkin IM, Cornillon PC, Sherman K (2009)** Fronts in Large Marine Ecosystems. *Progress in Oceanography* 81:223–236.
- Benitez-Nelson C, Mcgillicuddy D (2008)** Mesoscale physical-biological-bio-geochemical linkages in the open ocean: An introduction to the results of the E-Flux and EDDIES programs - Preface. *Deep Sea Research Part II Topical Studies in Oceanography* 55.
- Block BA, Dewar H, Blackwell SB, Williams TD, Prince ED, Farwell CJ, Boustany A, Teo SL, Seitz A, Walli A, Fudge D (2001)** Migratory movements, depth preferences, and thermal biology of Atlantic bluefin tuna. *Science* 293:1310–1314.
- Carr A (1987)** New Perspectives on the Pelagic Stage of Sea Turtle Development. *Conservation Biology* 1:103–121.
- Carr A, Meylan AB (1980)** Evidence of passive migration of green turtle hatchlings in sargassum. *Copeia* 1980:366–368.
- Casazza TL, Ross SW (2008)** Fishes associated with pelagic Sargassum and open water lacking Sargassum in the Gulf Stream off North Carolina. <http://aquaticcommons.org/id/eprint/8817>.
- CBD (2012)** Report of the Wider Caribbean and Western Mid-Atlantic Regional Workshop to Facilitate the Description of Ecologically or Biologically Significant Marine Areas, Recife, 28 February - 2 March 2012, 241 pp. Convention on Biological Diversity Document UNEP/CBD/SBSTTA/16/INF/7
- Cornillon P (2007)** Fronts in the World Ocean's Large Marine Ecosystems. 21.
- Cornillon P, Evans D, Large W (1986)** Warm outbreaks of the Gulf Stream into the Sargasso Sea. *Journal of Geophysical Research: Oceans* 91:6583–6596.
- Coston-Clements L, Settle LR, Hoss DE (no date)** Utilization of the Sargassum habitat by marine invertebrates and vertebrates, a review.
- Cummings JA, Smedstad OM (2013)** Variational Data Assimilation for the Global Ocean. In: *Data Assimilation for Atmospheric, Oceanic and Hydrologic Applications (Vol. II)*. Park SK, Xu L (eds) Springer, Berlin, Heidelberg, p 303–343
- Dooley J (1972)** Fishes associated with the pelagic Sargassum complex, with a discussion of the Sargassum community. *Contrib Mar Sci* 16:1–32.
- Gunn, J.T., and D.R. Watt, 1982:** On the currents and water masses north of the Antilles/Bahamas Arc, *Journal of Marine Research*, 40, 1–48.
- Friedland KD, Miller MJ, Knights B (2007)** Oceanic changes in the Sargasso Sea and declines in recruitment of the European eel. *ICES Journal of Marine Science* 64:519–530.
- GHR SST Level 4 MUR Global Foundation Sea Surface Temperature Analysis (v4.1) (no date)** <https://podaac.jpl.nasa.gov/dataset/MUR-JPL-L4-GLOB-v4.1> (accessed December 1, 2022)
- Kavanaugh MT, Oliver MJ, Chavez FP, Letelier RM, Muller-Karger FE, Doney SC (2016)** Seascapes as a new vernacular for pelagic ocean monitoring, management and conservation. *ICES J Mar Sci* 73:1839–1850.
- Kleckner RC, McCleave JD, Wippelhauser GS (1983)** Spawning of American eel, *Anguilla rostrata*, relative to thermal fronts in the Sargasso Sea. *Environ Biol Fish* 9:289–293.
- Laffoley, D. d'A., Roe, H. S. J., Angel, M. V., Ardron, J., Bates, N. R., Boyd, I. L., Brooke, S., Buck, K. N., Carlson, C. A., Causey, B., Conte, M. H., Christiansen, S., Cleary, J., Donnelly, J., Earle, S.A., Edwards, R., Gjerde, K.M., Giovannoni, S. J., Gulick, S., Gollock, M., Hallett, J., Halpin, P., Hanel, R., Hemphill, A., Johnson, R. J., Knap, A. H., Lomas, M. W., McKenna, S. A., Miller, M. J., Miller, P. I., Ming, F. W., Moffitt, R., Nelson, N. B., Parson, L., Peters, A. J., Pitt, J., Rouja, P., Roberts, J., Roberts, J., Seigel, D.A., Siuda, A. N. S., Steinberg, D. K., Stevenson, A., Sumaila, V. R., Swartz, W., Thorrold, S., Trott, T. M., Vats, V. (2011)** The protection and management of the Sargasso Sea: The golden floating rainforest of the Atlantic Ocean. Summary Science and Supporting Evidence Case. Sargasso Sea Alliance, Washington, DC.
- Laurindo LC, Mariano AJ, Lumpkin R (2017)** An improved near-surface velocity climatology for the global ocean from drifter observations. *Deep Sea Research Part I: Oceanographic Research Papers* 124:73–92.
- Loefer J, Sedberry G, McGovern J (2007)** Nocturnal Depth Distribution of Western North Atlantic Swordfish (*Xiphias gladius*, Linnaeus, 1758) in Relation to Lunar Illumination. *Gulf and Caribbean Research* 19:83–88.
- Lomas, M.W., Bates, N.R., Buck, K.N. and A.H. Knap. (eds) 2011a.** *Oceanography of the Sargasso Sea: Overview of Scientific Studies*. Sargasso Sea Alliance Science Report Series, No 5, 64 pp. ISBN 978-0-9847520-7-2
- Luckhurst BE, Prince ED, Llopiz JK, Snodgrass D, Brothers EB (2006)** Evidence of Blue Marlin (*Makaira nigricans*) Spawning in Bermuda Waters and Elevated. *Bulletin of Marine Science* 79:14.
- Mahadevan A (2014)** Eddy effects on biogeochemistry. *Nature* 506:168–169.

**Mansfield KL, Wyneken J, Luo J (2021)** First Atlantic satellite tracks of 'lost years' green turtles support the importance of the Sargasso Sea as a sea turtle nursery. *Proceedings of the Royal Society B: Biological Sciences* 288:20210057.

**Mansfield KL, Wyneken J, Porter WP, Luo J (2014)** First satellite tracks of neonate sea turtles redefine the 'lost years' oceanic niche. *Proceedings of the Royal Society B: Biological Sciences* 281:20133039.

**Miller MJ, Westerberg H, Sparholt H, Wysujack K, Sørensen SR, Marohn L, Jacobsen MW, Freese M, Ayala DJ, Pohlmann J-D, Svendsen JC, Watanabe S, Andersen L, Møller PR, Tsukamoto K, Munk P, Hanel R (2019)** Spawning by the European eel across 2000 km of the Sargasso Sea. *Biology Letters* 15:20180835.

**NASA Goddard Space Flight Center, Ocean Ecology Laboratory, Ocean Biology Processing Group; (2014):** MODIS-Aqua Ocean Color Data; NASA Goddard Space Flight Center, Ocean Ecology Laboratory, Ocean Biology Processing Group. [http://dx.doi.org/10.5067/AQUA/MODIS\\_OC.2014.0](http://dx.doi.org/10.5067/AQUA/MODIS_OC.2014.0)

**National Marine Fisheries Service (2010)** Final recovery plan for the sperm whale (*Physeter macrocephalus*). National Marine Fisheries Service, Silver Springs, MD.

**Pegliasco C, Delepouille A, Mason E, Morrow R, Faugère Y, Dibarboure G (2022)** META3.1exp: a new global mesoscale eddy trajectory atlas derived from altimetry. *Earth System Science Data* 14:1087–1107.

**Politis SN, Syropoulou E, Benini E, Bertolini F, Sørensen SR, Miest JJ, Butts IAE, Tomkiewicz J (2021)** Performance thresholds of hatchery produced European eel larvae reared at different salinity regimes. *Aquaculture* 539:736651.

**RStudio Team (2020).** RStudio: Integrated Development for R. RStudio, PBC, Boston, MA URL <http://www.rstudio.com/>.

**Richardson PL, Cheney RE, Worthington LV (1978)** A census of Gulf Stream rings, spring 1975. *Journal of Geophysical Research: Oceans* 83:6136–6144.

**Roberts JJ, Best BD, Dunn DC, Trembl EA, Halpin PN (2010)** Marine Geospatial Ecology Tools: An integrated framework for ecological geoprocessing with ArcGIS, Python, R, MATLAB, and C++. *Environmental Modelling & Software* 25:1197–1207.

**Skomal GB, Zeeman SI, Chisholm JH, Summers EL, Walsh HJ, McMahon KW, Thorrold SR (2009)** Transequatorial Migrations by Basking Sharks in the Western Atlantic Ocean. *Current Biology* 19:1019–1022.

**South Atlantic Fishery Management Council (2002)** Fishery Management Plan for Pelagic Sargassum Habitat of the South Atlantic Region. South Atlantic Fishery Management Council, Charleston, SC.

**Taburet G, Sanchez-Roman A, Ballarotta M, Pujol M-I, Legeais J-F, Fournier F, Faugere Y, Dibarboure G (2019)** DUACS DT2018: 25 years of reprocessed sea level altimetry products. *Ocean Science* 15:1207–1224.

**Wright D, Sayre R, Breyer S, Butler K, VanGraafeiland K, Costello M, Goodin K, Kavanaugh M, Cressie N, Basher Z, Harris P, Guinotte J (2018)** Ecological Marine Units as a framework for collaborative data science and knowledge discovery.







FONDS FRANÇAIS POUR  
L'ENVIRONNEMENT MONDIAL